

**GROWTH AND ELECTRICAL
CHARACTERIZATION OF HIGH PURITY
CARBON NANOTUBES**

**A Thesis submitted to
The graduate school of engineering and science of
İzmir Institute of Technology
In partial Fulfillment of the Requirement for the Degree of**

MASTER OF SCIENCE

In Physics

**by
Serap KIR**

**June 2009
İZMİR**

We approve the thesis of **Serap KIR**

Assist. Prof. Yusuf SELAMET

Supervisor

Assoc. Prof. Lütfi ÖZYÜZER

Co-Supervisor

Assist. Prof. Savaş BERBER

Committee Member

Assoc. Prof. R. Tuğrul SENGER

Committee Member

Assoc. Prof. Enver TARHAN

Committee Member

June 25, 2009

Prof. Durmuş Ali DEMİR

Head of the Physics Department

Prof. Hasan BÖKE

Dean of the Graduate
School of Engineering and Science

ACKNOWLEDGEMENT

I would like to express my gratitude to all those who gave me the possibility to complete this thesis. Firstly, I would like to thank my supervisor Assist Prof Yusuf Selamet for his instructive guidance and encouragement during this thesis study. Also, I thank Assoc Prof Lütfi Özyüzer for making me motivated not only during master education but also during undergraduate education. Moreover, I would like to thank Assist Prof Süleyman Tari for growing our catalyst thin films. Furthermore, I thank Assoc Prof Salih Okur for his positive attitude all the time. I thankfully acknowledge TUBITAK for financial support during this project (TUBITAK TBAG-105T462). Additionally, I am thankful to my lab mates and friends at IYTE for their motivation and nice friendship. Finally, I am very thankful to my family for their financial support, comments and motivation in all my life.

ABSTRACT

GROWTH AND ELECTRICAL CHARACTERIZATION OF HIGH PURITY CARBON NANOTUBES

This thesis work is focused on growing high purity vertically aligned Carbon nanotubes by ethylene gas thermal chemical vapor deposition method on very thin Cobalt and Iron catalyst thin films deposited on to Si/SiO₂/Al₂O₃ substrates by DC magnetron sputtering. In this study, the effective parameters were changed to grow aligned CNTs. Hence, the vertically aligned CNTs were performed and also the ideal parameters were determined for this kind of growth mechanism.

The effect of support layer was examined for three different hydrocarbon gas ratios. SiO₂ and Al₂O₃ were used as support layers between metal catalyst thin films and Si substrate. Two kinds of samples were compared; one of them had only Al₂O₃ and the other one includes both Al₂O₃ and SiO₂ layers. As a result, the sample that had both oxide layers gave better results for density of CNTs on the surface of samples.

Moreover, types of catalyst material effect also were examined on growth of CNTs for three different temperatures. For this aim, the performance of Fe and Co catalyst thin films was compared. According to our results, Fe was more reactive with ethylene gas than Co catalysts and also, the density of CNTs was increased by using Fe as a catalyst material.

Hydrogen pretreatment time was performed for another significant effect. Seven different time parameter which were 0, 5, 10, 15, 20, 25, 30 minutes, were examined. The density and diameters of catalysts particles were compared for these different treatment times.

Finally, the electrical characterization of CNTs was performed. The resistance of CNTs was measured by using two point contact technique. Moreover, the interaction between resistance of CNTs and humidity was examined.

ÖZET

YÜKSEK SAFLIKTA KARBON NANOTÜPLERİN BÜYÜTÜLMESİ VE ELEKTRİKSEL KARAKTERİZASYONU

Bu tez çalışması, yüksek saflıkta dikey karbon nanotüplerin etilen gazı termal kimyasal buhar biriktirme tekniği ile doğru akım mıknatıssal saçtırma yöntemiyle silikon dioksit üzerine alüminyum oksit kaplanmış silikon alt taşları üzerine kaplanan Kobalt ve Demir ince kataliz filmlerin üzerinde büyütülmesine odaklanmıştır. Bu çalışmada dikey karbon nanotüpleri büyütme için etkili parametreler değiştirilmiştir. Böylece, dikey nanotüpler oluşturulmuş ve uygun parametrelere karar verilmiştir.

Ayrıca, tampon tabakasının etkisi üç farklı oranda karbon gazı için araştırılmıştır. SiO_2 ve Al_2O_3 silikon ve metal kataliz ince film arasında tampon tabakası olarak kullanılmışlardır. İki farklı örnek karşılaştırılmıştır. Bir çeşit örnek sadece Al_2O_3 tampon tabakası içerirken, diğer çeşit SiO_2 ve Al_2O_3 tabakalarına sahiptir. Sonuç olarak iki oksit tabakasını içeren örnek çeşidinin karbon nanotüplerin yüzeydeki yoğunlukları için daha iyi olduğu anlaşılmıştır.

Kataliz maddenin çeşidinin karbon nanotüpler üzerindeki etkisi de üç farklı sıcaklık için incelendi. Bu amaç için, Demir ve Kobalt ince filmlerin performansları karşılaştırıldı. Sonuçlara göre, Demir parçacıklar etilen gazı ile Kobalt parçacıklarına göre daha aktiftir ayrıca, karbon nanotüplerin yüzey yoğunlukları Demir kataliz kullanılarak artırılmıştır.

Hidrojen önışlem etkisi de diğer bir önemli parametre olarak uygulandı. 0, 5, 10, 15, 20, 25, 30 dakika olarak yedi farklı zaman değeri denenmiştir. Kataliz parçacıkların yoğunlukları ve yarıçapları bu farklı zaman uygulamaları için karşılaştırıldı.

Son olarak, karbon nanotüplerin elektriksel karakterizasyonu yapılmıştır. İki nokta kontak modeli kullanılarak tüplerin dirençleri ölçülmüştür. Ek olarak, karbon nanotüplerin nem ile olan ilişkisi de incelenmiştir.

TABLE OF CONTENT

LIST OF FIGURES	VIII
LIST OF TABLES.....	XI
CHAPTER 1. INTRODUCTION.....	1
CHAPTER 2. CARBON NANOTUBES	3
2.1. Carbon Structures.....	3
2.2. Carbon Nanotubes	4
2.2.1. Historical Background.....	4
2.2.2. Types of Carbon Nanotubes	5
2.2.2.1. Single Wall Carbon Nanotube.....	5
2.2.2.2. Multi-Wall Carbon Nanotube.....	6
2.2.3. Classification of Carbon Nanotubes.....	6
2.3. Carbon Nanotube Synthesis Methods	8
2.3.1. Arc-Discharge Method.....	8
2.3.2. The Laser –Furnace Method.....	9
2.3.3. Chemical Vapor Deposition Method.....	11
2.4. Growth Mechanism of CNTs	12
CHAPTER 3. THE CATALYST	15
3.1. Catalyst Thin Film.....	15
3.2. Thin Film Support Layer.....	18
CHAPTER 4. EXPERIMENTAL	19
4.1. DC Magnetron Sputtering Process.....	19
4.2. Thermal Chemical Vapor Deposition with CNT Growth Process.....	21
4.3. Characterization Techniques	22
4.3.2. Transmission Electron Spectroscopy	23

4.3.3. Atomic Force Microscopy	24
CHAPTER 5. RESULTS AND DISCUSSIONS	25
5.1. SEM and AFM Results	25
5.1.1. Growth of Aligned Carbon Nanotubes.....	25
5.1.2. Support Layer Effect on the CNT Growth	28
5.1.3. Catalyst Thin Film Effect on the CNT Growth.....	30
5.1.4. H ₂ Pretreatment Time Effect on CNT Growth.....	36
5.2. TEM Results.....	41
5.3. Electrical Measurement Results.....	45
CHAPTER 6. CONCLUSION	54
REFERENCES	56

LIST OF FIGURES

<u>Figure</u>	<u>Page</u>
Figure 2.1. Diamond in the cubic form.....	3
Figure 2.2. C60 Buckminsterfullerene.....	4
Figure 2.3. Graphite structure	4
Figure 2.4. An illustration of a SWNT	6
Figure 2.5. An illustration of a MWNT	6
Figure 2.6. An illustration of unrolled graphene	7
Figure 2.7. Classification of CNTs a) Zig-zag b) Arm-chair c) Chiral CNTs.....	8
Figure 2.8. Simple schematic illustration of an arc-discharge apparatus	9
Figure 2.9. Schematic illustration of a laser ablation method	11
Figure 2.10. A schematic illustration of a CVD System	12
Figure 2.11. Schematic illustration of CNT growth mechanism	13
Figure 2.12. Schematic illustrations of Tip and Base growth mechanisms.....	14
Figure 3.1. Schematic illustration of catalyst nanoparticles orientation.....	16
Figure 3.2. SEM image of Fe catalyst particles.....	17
Figure 3.3. SEM image of Co catalyst particles	17
Figure 3.4. Growth model on a porous support layer	18
Figure 4.1. The TCVD system based in Physics Department, CNL Lab, IYTE	20
Figure 4.2. a) Quartz boat, b) Some thin films used for CNT growth.....	20
Figure 5.1. SEM micrographs of a) FeAl10CNT 258 b) FeAl06CNT 254 c) FeAl08CNT 245 d) FeAl05CNT 238 e) FeAlCNT 232 f) FeAl06CNT 235	26
Figure 5.2. SEM micrographs of a) FeAl08CNT256 b) FeAl08CNT256 c) FeAl09CNT257d) FeAl09CNT257e) FeAlCNT263 f) FeAl08CNT263 ...	27
Figure 5.3. SEM micrographs of, a) FeAl06CNT261 b) FeAl10CNT 265 with 150/140 C ₂ H ₄ /H ₂ ratio.....	29

Figure 5.4. SEM micrographs of, a) FeAl06CNT 254 b) FeAl10CNT 258 with 180/140 C ₂ H ₄ /H ₂ ratio.....	29
Figure 5.5. SEM micrographs of, a) FeAl06CNT 333 b) FeAl10CNT 332 with 210/140 C ₂ H ₄ /H ₂ ratio.....	30
Figure 5.6. SEM micrographs of, a) FeAl08CNT 319 b) FeAl08CNT 319 c) CoAl01CNT 334 d) CoAl01CNT 334 at 750 °C with 20000X and 50000X magnification.....	31
Figure 5.7. SEM micrographs of, a) FeAl08CNT 356 b) FeAl08CNT 356 c) CoAl01CNT 355 d) CoAl01CNT 355 at 700 °C with 20000X and 50000X magnification.....	32
Figure 5.8. SEM micrographs of, a) FeAl08CNT 347 b) FeAl08CNT 347 c) CoAl01CNT 348 d) CoAl01CNT 348 at 650 °C with 20000X and 50000X magnification.	33
Figure 5.9. AFM micrographs of, a) FeAl08 357 b) CoAl01 358 at 650 °C.....	35
Figure 5.10. AFM micrographs of, a) FeAl08 362 b) CoAl01 363 at 700 °C.....	35
Figure 5.11. AFM micrographs of a) FeAl08 322 b) CoAl01 364 at 750 °C.....	36
Figure 5.12. AFM micrographs of a) FeAl08 316 b) FeAl08 316 0 min. Treatment time.....	37
Figure 5.13. AFM micrographs of a) FeAl08 306 b) FeAl08 306 5 min. Treatment time.....	38
Figure 5.14. AFM micrographs of a) FeAl08 303 b) FeAl08 303 10 min. Treatment time.....	38
Figure 5.15. AFM micrographs of a) FeAl08 322 b) FeAl08 322 15 min. Treatment time.....	39
Figure 5.16. AFM micrographs of a) FeAl08 326 b) FeAl08 326 20 min. Treatment time.....	39
Figure 5.17. AFM micrographs of a) FeAl08 313 b) FeAl08 313 25 min. Treatment time.....	40
Figure 5.18. AFM micrographs of a) FeAl08 329 b) FeAl08 329 30 min. Treatment time.....	40
Figure 5.19. TEM micrographs of FeAl09CNT264 with different magnifications.....	42
Figure 5.20. Three TEM micrographs of FeAl08CNT296 with different magnifications.....	43

Figure 5.21. TEM micrographs of, a) FeAlO8CNT 256 b) FeAl10CNT 269 c) FeAlO8CNT 273 d) FeAlO9CNT 277	44
Figure 5.22. Photo of gold electrode with CNTs	46
Figure 5.23. SEM micrographs of gold electrode with CNTs with different magnifications	46
Figure 5.24. Resistance –Humidity graph of empty gold electrode	47
Figure 5.25. Resistance –Humidity graph of FEAlO9CNT 297.....	47
Figure 5.26. Resistance –Humidity graph of FEAlO9CNT297 for along time	48
Figure 5.27. Current-Voltage (I-V) graph of FEAlO9CNT 297.....	49
Figure 5.28. Resistance –Humidity graph of FEAlO9CNT273.....	49
Figure 5.29. Resistance –Humidity graph of FEAlO9CNT297 with different ratio of humidity	50
Figure 5.30. Current-Voltage (I-V) graph of FEAlO9CNT 273.....	51
Figure 5.31. Resistance –Humidity graph of FEAlO8CNT 276.....	51
Figure 5.32. Resistance –Humidity graph of FEAlO8CNT 283.....	52
Figure 5.33. Current-Voltage (I-V) graph of FEAlO8CNT 283.....	53

LIST OF TABLES

<u>Table</u>	<u>Page</u>
Table 4.1. Growth conditions of CNTs for TCVD method	22
Table 5.1. Growth parameters of some steps to have vertical CNTs.....	28
Table 5.2. Growth parameters of CNTs on Fe and Co catalyst thin films.....	34
Table 5.3. Growth parameters of Fe and Co catalyst nano particles	34
Table 5.4. Growth conditions of catalyst particles for TCVD method.....	37
Table 5.5. Parameters of CNTs which have TEM results	42

CHAPTER 1

INTRODUCTION

Since the early 90s, many scientists have focused on a new topic which is one of the fascinating carbon materials. It is called carbon nanotube (CNT). Several experiments have been done and hundreds of papers have been published to determine the growth parameters, the characterization methods and also the application areas of CNTs. This discovery creates a new era, which is expanding with huge steps rapidly.

A graphite sheet (graphene) rolls into a cylinder and it creates a carbon nanotube which has excellent properties due to its rolling dimension and symmetric structure. For nanoscience, CNTs have very significant value not only for their mechanical, electronics and well defined atomic structural properties but also for their potential technological applications in electronic devices and in the field of hydrogen storage and these properties separate CNTs from other materials (Jodin, et al. 2006).

There are two types of carbon nanotubes; if it contains one graphene cylinder, it is named single wall nanotube (SWNT); if it contains more than one concentric cylinders, it is called multi wall carbon nanotube (MWNT) (Dresselhaus, et al. 2001). Although graphene is a zero-gap semiconductor, CNTs can be semiconductors or metals with different size energy gaps (Dresselhaus, et al. 2004). The types of CNTs can give some information about their electrical properties. The (n, m) values define the SWNT is metallic or not. Nanotube with $(n-m) = 3q$ is metallic and the tube with $(n-m) = 3q+1$ is semiconducting (q is an integer). These (n, m) values are related to the chiral vector $(C = n\hat{a}_1 + m\hat{a}_2)$, C is chirality vector). SWNTs are classified into three groups; armchair, zigzag and chiral, and these groups are revealed with these n, m values (Ivchenko and Spivak 2002). If $n=m$ nanotube is called armchair and if $m=0$ it is zigzag, finally n is not equal m , it is chiral (Belin and Epron 2005). Although zigzag nanotubes are to be either semiconducting or metallic, all armchair nanotubes are metallic nanotubes (Saito, et al. 1992).

In a graphene layer, the carbon-carbon bond probably is the strongest chemical bond, so it makes SWNTs the toughest materials ever known. This SWNT is 100 times

stronger than steel because of this C-C bonds (Baughman, et al. 2002, Dresselhaus, et al.2004). The Young's modulus of SWNT is up to 1 TPa, which is 5 times greater than the value for steel (230 GPa) while the density is only 1.3 g/cm³ (Saito, et al. 1992). Despite the high Young's modulus of CNTs, they can be bended reversibly up to a critical angle value as large as 110° (Folvo, et al. 1997, Iijima, et al. 1996). In the literature, there is not as much as publication about the thermal properties including thermal conductivity, thermo power, specific heat of CNTs than the other papers which explain the electronic, mechanical properties (Dresselhaus, et al.2004).

To grow CNTs, catalyst materials have a significant position. The groups around the world share the same idea that the three transition metals Fe, Co and Ni and also the compounds of these metals are the best catalysts for CNTs. (Dai 2002). These metals (Fe, Co, Ni) have finite carbon solubility at high temperatures (Dai 2002, Park, et al. 2002).

This thesis is focused on optimizing the parameters to grow vertical CNTs by ethylene thermal chemical vapor deposition and to investigate some main parameters affecting the growth of CNTs, such as catalyst, pretreatment time, and support layer thickness effects. This thesis is composed of six chapters. Chapter 2 gives background information on CNTs, their types, structure, discovery and growth methods along with growth mechanisms. In Chapter 3, general information about catalyst materials and the catalyst thin film and also a short literature survey are mentioned. The growth of catalyst thin films, experimental conditions, and the characterization techniques are mentioned in Chapter 4. The next chapter is discussion part, all experimental details and characterization results are shown in Chapter 5. Chapter 6 is the last one, which is conclusion.

CHAPTER 2

CARBON NANOTUBES

2.1. Carbon Structures

Carbon is the basis of organic life, and it is a unique active element not only for academic research but also for potential applications. It is easy for a carbon atom to bond with many elements such as nitrogen, hydrogen, oxygen, and also a carbon atom can bond with another carbon atom in several configurations (Bonard 2006). The forms of carbon are diamond, fullerene, graphite, and also carbon nanotubes.

Diamond is one of the best known allotropes of carbon, it is reformed from graphite at high temperature and at high pressure, and it is the hardest form of carbon and the other material. It is used in industry to grind and cut and polish materials.

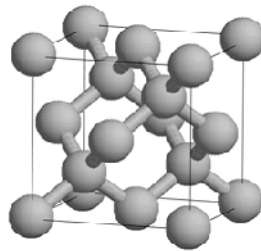


Figure 2.1. Diamond in the cubic form
(Source: Stahl 2000)

The other form of carbon can contain 60, 70 or 82 carbon atoms. They are closed spheres composed of pentagons and hexagons. The curvature of shape is given by these hexagons and pentagons so it is like a ball, and is called fullerene. In 1985, the fullerene form of carbon was discovered by laser vaporization of graphite target (Kroto, et al.1985, Belin and Epron 2005).

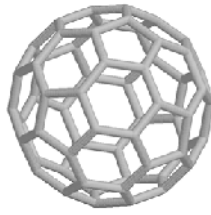


Figure 2.2. C60 Buckminsterfullerene
(Source: Stahl 2000)

The most stable form of carbon at room temperature and atmospheric pressure is graphite (Baddour and Briens 2005). Graphite is able to conduct electricity. It is chemically more reactive than diamond. A single layer of graphite is called graphene which has remarkable electrical, thermal, and physical properties.

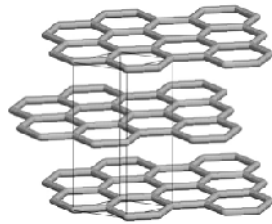


Figure 2.3. Graphite structure
(Source : Stahl 2000)

The last one, which we focused on in this study is carbon nanotube (CNT) which is going to be described in the following step.

2.2. Carbon Nanotubes

2.2.1. Historical Background

Carbon nanotube is a tubular form of a graphene with a diameter in the range of the nanometer . In 1950s, the electron microscopes started to become famous for a wide

research area and the tubular form of carbon was first observed using an electron microscope by Russian researchers Radushkevich and Lukyanovich in 1952, it was called carbon filament (Dupuis 2005, Monthieux and Kuznetsov 2006).

In the early 90s, Sumio Iijima who is an electron microscopist was performing some experiments to observe fullerene and allotropes of it. However, he noticed that different forms were occurred like a tubular structures of carbon . After this coincidence, this carbon filaments have been called carbon nanotubes (CNTs)(Dupuis 2005).

The first CNTs were multi-wall carbon nanotubes (MWCNTs), which were grown by Arc-discharge process and only two years later single-wall carbon nanotubes could be grown by two different methods; such as laser ablation method and chemical vapor deposition (CVD) (Dupuis 2005, Iijima and Ichihashi 1993).

2.2.2 Types of Carbon Nanotubes

The number of the concentric graphene cylinders determine the types of carbon nanotubes. If carbon nanotube contains one graphene cylinder, it is named single wall nanotube (SWNT); if it contains more than one concentric cylinder, it is called multi wall carbon nanotube (MWNT).

2.2.2.1 Single Wall Carbon Nanotube

A graphene rolls into a cylinder and single-wall carbon nanotube is occurred which has excellent mechanical, electronical and well defined atomic structural properties (Jodin, et al. 2006). A single wall carbon nanotube can be metallic or semiconductor.

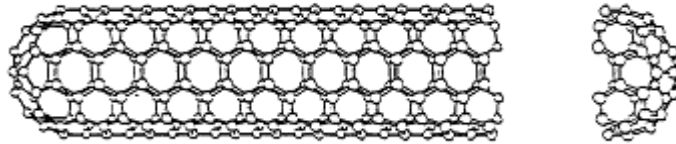


Figure 2.1. An illustration of a SWNT
(Source : Dresselhaus 1998)

2.2.2.2. Multi-Wall Carbon Nanotube

More than one concentric graphene cylinders form into multi-wall carbon nanotube . Although MWNTs are stronger than SWNTs , they have more defects than SWNTs (Dai 2002). MWNTs have not been characterized in detail for their physical properties because of the difficulty of making measurements on the individual shells of the nanotube.

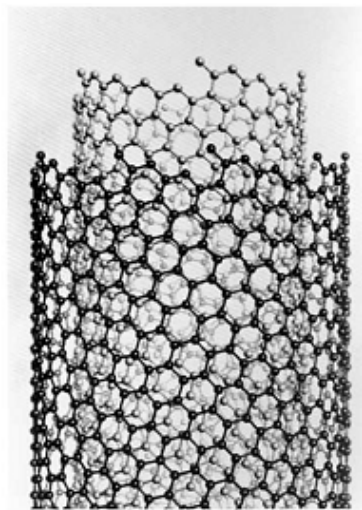


Figure 2.5. An illustration of a MWNT
(Source : Iijima 1991)

2.2.3. Classification of Carbon Nanotubes

When a graphene sheet rolls into tubular form, the structure can be in three different configuration such as; armchair carbon nanotube, zigzag carbon nanotube and

finally chiral carbon nanotube. The orientation of chiral vector ($\vec{C} = n\hat{a}_1 + m\hat{a}_2$, \vec{C} is chirality vector) determines the atomic structure of tubes. These (n, m) values are related to the chiral vector and also the chiral angle (θ) gives information about orientations of CNTs. The chiral angle (θ), as shown in Figure 2.6, is defined as the angle between the vectors C and \hat{a}_1 , with values of θ in the range of $0 \leq \theta \leq 30$.

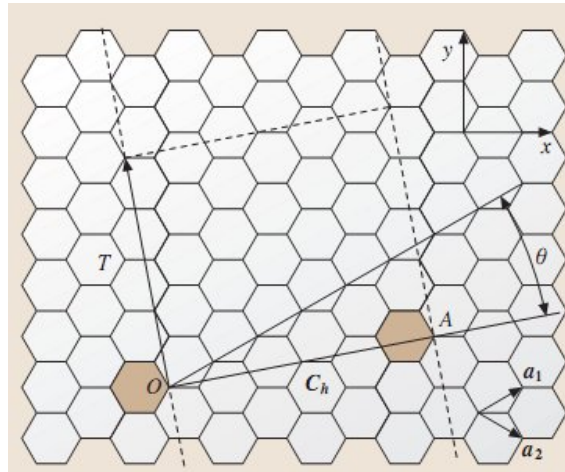


Figure 2.6. An illustration of unrolled graphene
(Source : Hamada, et al. 1992)

When $n=m$ CNT is called armchair type $\theta=0^\circ$, if $m=0$ CNT is zigzag $\theta=30^\circ$, finally $n \neq m$ the tube is chiral $0 < \theta < 30^\circ$ (Belin and Epron 2005). The classifications of CNTs are depicted in Figure 2.7. The zigzag and armchair carbon nanotubes, as are shown in Fig.2.8.(a) and (b), respectively, have mirror images which have identical structure to the originals; Chiral nanotubes exhibit a spiral symmetry whose mirror image cannot be superposed on to the original one.

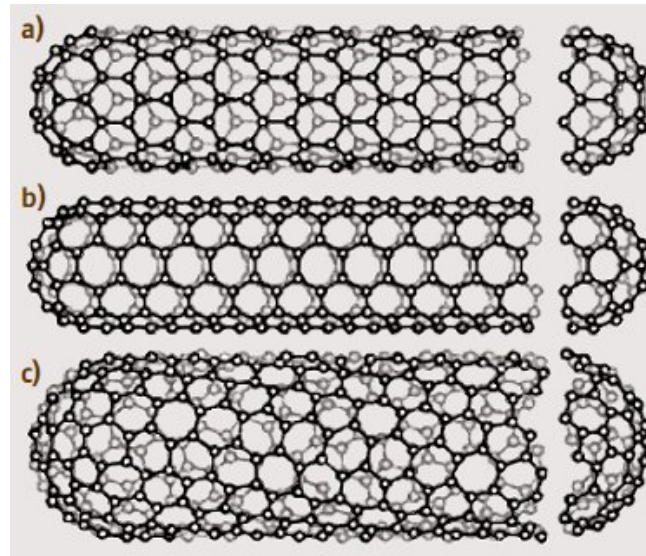


Figure 2.7. Classification of CNTs a) Zig-zag b) Arm-chair c) Chiral CNTs
(Source : Dresselhaus, et al. 1995)

2.3. Carbon Nanotube Synthesis Methods

Three growth techniques are the most general for CNTs. One of them is arc-discharge method and also it is the first one, second one is furnace ablation method and most suitable one for SWNTs, the last one is chemical vapor deposition technique. All the methods have characteristic features and they have advantages and also disadvantages. Each technique is shortly explained below.

2.3.1. Arc-Discharge Method

The Arc-discharge method is the first one and the easiest one to use for producing carbon nanotubes (Iijima 1991). This method involves the CNT growing on carbon electrodes (cathode and anode) by applying DC (direct current) during arc-discharge evaporation of carbon in an inert buffer gas such as argon or helium (Popov 2004).

Furthermore, in this method, there are two high-purity graphite electrodes. When a graphite electrode contains catalyst such as Fe, Co, Ni, it is called anode; the other one is pure and is used as a cathode (Iijima, et al. 1993). At low pressure (between 50 and 700 mbar) and in an ambient gas atmosphere, DC arc voltage is applied between two separate graphite rod (Ando, et al. 1993). The anode surface is heated to higher temperature such as 4000 °K, it causes anode to vaporize and condense on cathode surface so nano particles are occurred.

This process is occurred in an inert gas atmosphere and also can be applied in methane atmosphere. It was founded that methane is the best gas for growing of MWNTs (Ando 1994). It is proved that the CNTs can also be grown in the liquid nitrogen atmosphere or in water.

The pressure of inert gas during arc-evaporation process has an important and strong influence on SWCNTs. Moreover, the other significant parameter is the stability of electric arc during experiment (Harris 2007).

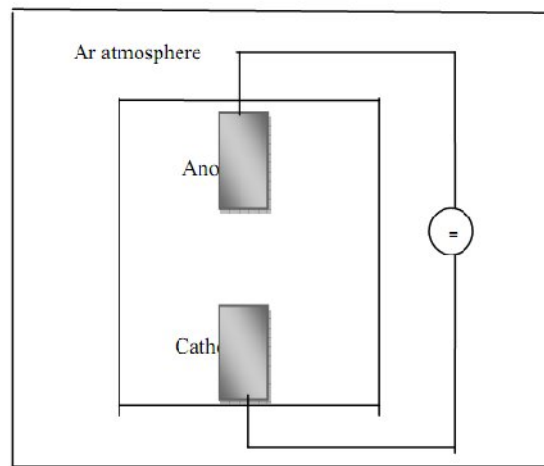


Figure 2.8. Simple schematic illustration of an arc-discharge apparatus
(Source : Popov 2004)

2.3.2. The Laser –Furnace Method

The laser furnace method or laser ablation method works with the same principle as arc- discharge method: Firstly evaporation of carbon gas and it is followed

by condensation (Rasmussen 2005). At high temperature nearly 1200°C, the furnace is heated and the flowing of an inert gas (typically argon or helium) passes through the tube. At this high temperature, a continuous or a pulse laser is used to vaporise the target which is located in the center of quartz tube furnace to produce fullerenes and CNTs. The target also consists of a mixture of graphite and metal catalysts, such as Fe, Co and Ni (Yudasaka, et al. 1999, Kataura, et al. 2000). For materials that have high boiling temperature, the laser can be more suitable than the other vaporization devices because of the energy density of laser (Guo, et al. 1995).

The principle of occurring a CNT is following these steps: Firstly, the target is vaporised and then a cloud is occurred which contain C, C₂, C₃ and rapidly catalyst vapors is formed. While the condensation of the cloud, the small weight of carbon molecules come together to form a larger one. The vaporized catalysts are included in this large molecule to prevent the closing of these carbon molecules into cage structure. The growth process is finalised with a SWNT. When the system is cooled up to low temperature, this process is finished (Scott, et al. 2001, Baddour and Briens 2005).

Since 1995, the laser ablation methods have been used to produce CNTs (Guo, et al. 1995). CNTs which have good quality have been produced by this method, however, the high temperatures and using laser makes this method a bit costly compared to other methods. A typical illustration of a laser-ablation method is depicted in Figure 2.9.

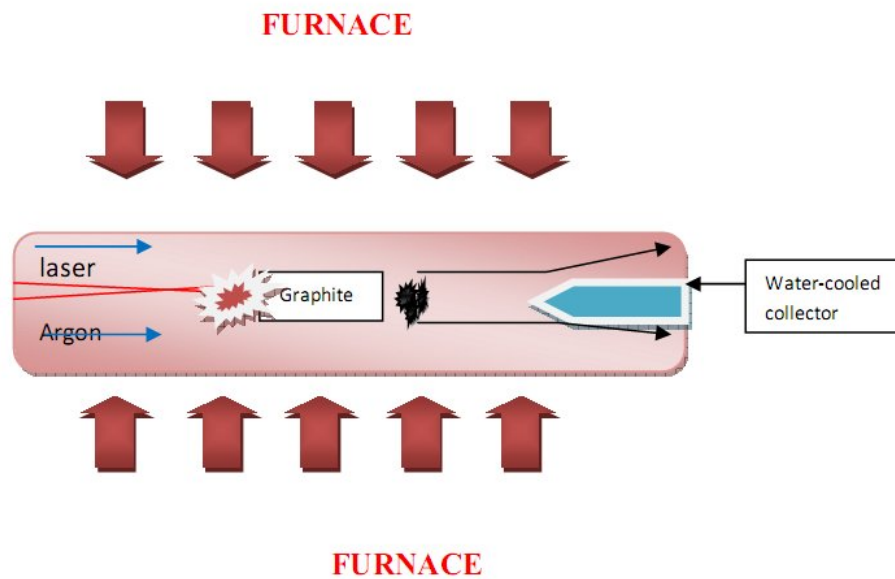


Figure 2.9. Schematic illustration of a laser ablation method
(Source : Guo, et al. 1995)

2.3.3. Chemical Vapor Deposition Method

Chemical vapor deposition technique was first used to grow CNTs, after two years of observing MWNTs by Iijima in 1991. Also CVD method has been used for producing carbon fiber and filaments since 1959 (Walker, et al. 1959, Dai 2002).

There are some reasons that why CVD is generally used to growth CNTs. Firstly, this method is performed at low temperature and also the size of CNTs can be controlled by controlling catalyst nanoislands (Weifeng, et al. 2003). Moreover, it is easy to perform and economic technique for synthesizing carbon nanotubes and also performing more than one sample at a time. The other reason is to be useful for large scale production of nanotube metaterials (Yamacan, et al. 1993, Weifeng, et al. 2003).

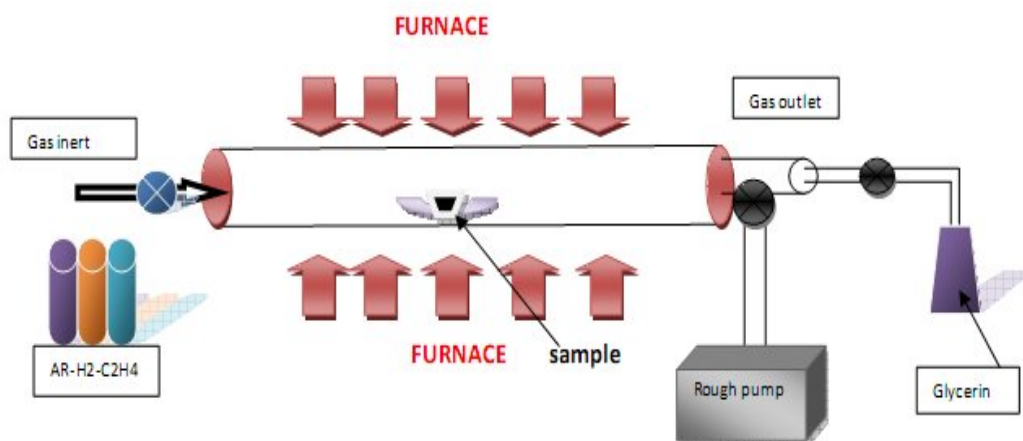


Figure 2.10. A schematic illustration of a CVD System
(Source : Journet and Barnier 1998)

Initially, the sample is placed in the quartz tube and the temperature is fixed for a selective point. During the increasing of the temperature, an inert gas (mostly Argon) flows through the tube to prevent the oxidation of samples and then. When the furnace reaches the selective temperature the etching gas (such as H_2 , NH_3) is started to flow through the tube to occur catalyst nano particles (Lee and Park 2001). The other step is sending hydrocarbon gas for decomposition of gas molecules on the catalyst surface and followed by diffusion of carbon through the catalyst particles. After that a carbon nanotube can be grow, by precipitation on catalyat surface. These hydrocarbon gases CH_4 , C_2H_4 , C_2H_2 , C_6H_6 , and Xylene can be used for a carbon source (Cui, et al. 2003)

Also CVD method has some difficulties about the characterization of carbon nanotubes because of mostly they are not aligned and not isolated after growth process (Li, et al. 1996).

2.4. Growth Mechanism of CNTs

In arc-discharge and laser ablation method, using catalyts is not necessary, however this is different for CVD method because mostly, a kind of metal catalys is

used to synthesis CNTs in this technique thus, the growth mechanism can be different for all these methods (Oberlin, et al.1976).

At present, the VLS (vapour-liquid-solid) model is the most acceptable one, in which the hydrocarbon molecules are broken and vapour carbon diffuses into nano-meter scale liquid catalyst particle, when the catalyst particle is filled with carbon, this carbon precipitates out with a graphitic structure (carbon filaments and CNTs)(Deck and Vecchio 2006, Ding and Balton 2006).The solubility of carbon in the catalyst is depending on the types of metal catalyst. The following figure shows the growth mechanism of CNTs.

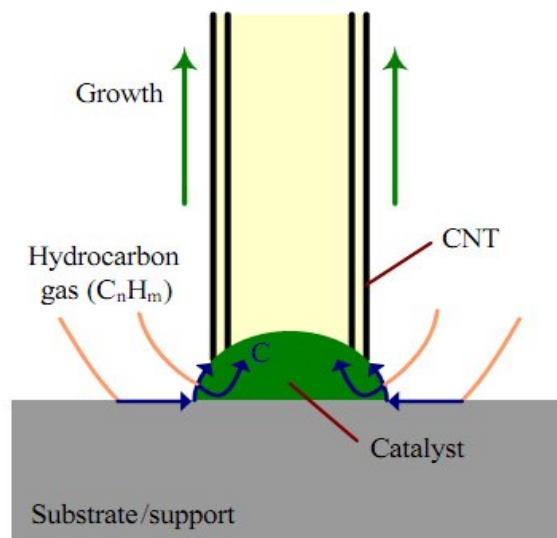


Figure 2.11. Schematic illustration of CNT growth mechanism (Source : Hart 2006)

In catalytic growth mechanism, the metal catalyst particle might stay at the end of the nanotube (tip growth) or the particle might sit of the starting end of CNT (base growth) (Dupuis 2005). For this modeling the interaction between the catalyst and support layer is so important. If the interaction is strong, it is base growth mechanism or it is weak, the mechanism is tip growth. Also the base growth model is more acceptable because the CNTs can be bended when the catalyst is end of the tube (tip growth) (Dupuis 2005). Figure 2.12 shows the types of growth mechanisms.

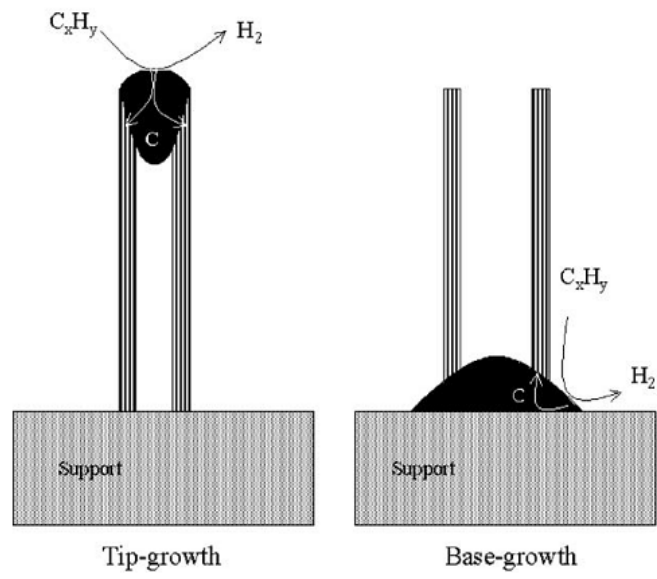


Figure 2.12. Schematic illustrations of Tip and Base growth mechanisms
(Source: Dupuis 2005)

CHAPTER 3

THE CATALYST

3.1. Catalyst Thin Film

In growing CNT, the catalyst material has very significant effect. The catalyst size and the catalyst density and also the types of catalyst directly affect the morphology, wall numbers, the diameter and also the growth mechanism of CNTs.

In general chemistry, the definition of catalyst is like this," a catalyst is a substance that increases the rate at which a chemical reaction approaches equilibrium without itself becoming permanently involved in the reaction." (Richardson 1989). When the hydrocarbon gas molecules diffuse into catalyst particle, metal carbides are occurred and when the catalyst is filled with carbon, this carbon precipitates out with a graphitic structure (carbon filaments and CNTs) (Deck and Vecchio 2006, Ding and Balton 2006). The metal catalyst particle might stay at the end of the nanotube (tip growth) or the particle might sit of the starting end of CNT (base growth)(Dupuis 2005). Following figure shows the possible probability of catalyst orientation during growth process.

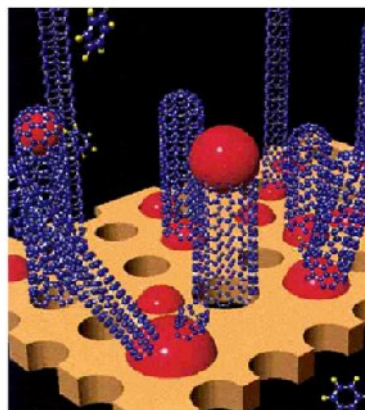


Figure 3.1. Schematic illustration of catalyst nanoparticles orientation
(Source : Dupuis 2005)

To determine the most suitable metal catalyst many experiments have been done, La, Cu, Gd, MgO, Ni, Co, Fe, Pd, Cr, Mn, Zn, Cd, Ti and Zr have been used for these experiments and Fe, Co and Ni and compounds of these transition metals give the best products. The type of catalyst on which CNT can grow, is called successful catalyst; otherwise, it is called unsuccessful catalyst. These metals (Fe, Co, Ni) have finite carbon solubility at high temperatures (Dai 2002, Park, et al. 2002). The carbon solubility limits of successful catalyst is between 0.5wt%-1.5wt% and if the carbon solubility is very close to zero and the metal carbides prevent the growing CNTs, these catalyst are renamed unsuccessful (Vecchio and Deck 2006).

Successful catalytic applications are found only in d-electron transition metals. It was also observed that the ability for transition metals to bond with carbon atoms increases with the number of unfilled d-orbitals (Arthur and Cho 1973). Alkali and alkaline metals revert too easily to ionic states under catalytic conditions (Richardson 1989). Moving from right to left across the periodic table means less d-electrons are available to fill the bonds of energies corresponding to collectivized d-orbitals. Levels are filled success until the Fermi level is reached. A certain number of vacant levels or d-holes are available for bonding with adsorbates; the lower the Fermi level the larger the number and stronger the adsorption (Richardson 1989).

These publications are samples of using Fe as a catalyst to growth CNT (Kukovecz, et al. 2000, Ermakova, et al. 2001, Pan SS, et al. 1999, Hernadi, et al. 1996, Fonseca, et al. 1996, Cui, et al. 2000, Wang YH, et al. 2001, Duesberg, et al. 2003, Klinke, et al. 2001, Ivanov, et al. 1994, Venegoni, et al. 2002, Fonseca, et al. 1996, Cui,

et al. 2000, Cho, et al. 2002, Duesberg, et al. 2003). In the following figure the Fe catalyst particles are shown.

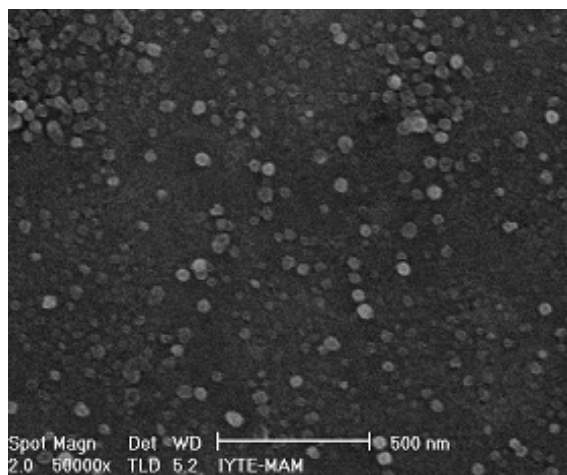


Figure 3.2. SEM image of Fe catalyst particles
(Source : Aksak, 2008)

The number of groups, doing experiment with Co catalyst, is lower than the others who are working on Fe and Ni catalysts (Dupuis 2005, Ivanov, et al. 1994, Hernadi, et al. 1996, Fonseca, et al. 1996, Ago, et al. 2000, Hsu, et al. 2002, Ago, et al. 2003, Dupuis 2005, Satishkumar, et al. 1998, Marty, et al. 2002, Colomer, et al. 1999, Colomer, et al. 2000).

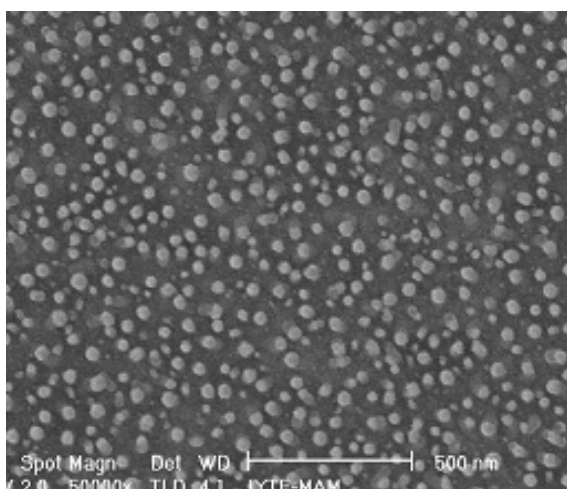


Figure 3.3. SEM image of Co catalyst particles
(Source : Aksak, 2008)

3.2. Thin Film Support Layer

The support layer is as important as catalyst nanoparticle for CNTs because the support layer affect the catalyst orientation and also the size of catalyst nanoparticles (Dai 2002). A buffer layer can act as a barrier between Si and the catalyst metal particles to prevent forming metal silicide (Arcos, et al. 2002, Teo, et al. 2002).

The support layer type is also important because it may cause different interactions between the supporting material and the catalyst metal. The interaction also affects the growth mechanism and the yields of CNTs (Qingwen, et al. 2002).

The most effective support material is porous one to produce catalyst nanoparticles with a suitable size for CNTs. High porous catalysts metal with strong metal-support interactions and high surface areas produce SWNTs with better and larger quantities. Strong metal interactions is important, it can prevent metal species from aggregating and unwanted large particles (Dai 2002).

The most common buffer layers are SiO_2 and Al_2O_3 . However, Alumina (Al_2O_3) is an electrical insulator, it has high thermal conductivity. In general, alumina is better than silica as a support layer for hydrocarbon CVD proces (Gaskell 1999). Figure 3.4 is a schematic for porous buffer layer.

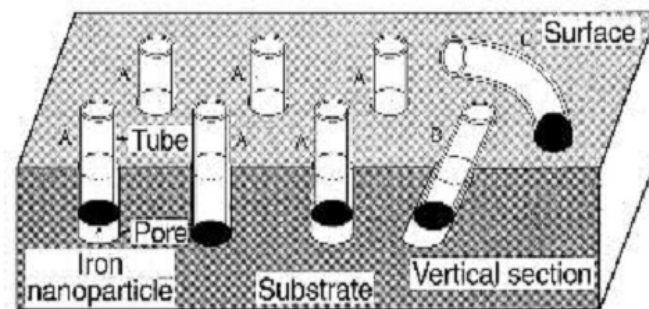


Figure 3.4. Growth model on a porous support layer
(Source : Li, et al. 1996)

Some example from literature for using alumina buffer layer(Cassell, et al. 1999, Colomer, et al. 1999, Maruyama, et al. 2002, Liu, et al.2003, Li, et al. 2003, Zhu, et al. 2003, Hiraoka, et al. 2003, Lyu, et al. 2003).

CHAPTER 4

EXPERIMENTAL

This chapter includes some main information about the experimental process. First section is devoted to DC magnetron sputtering process to grow catalyst thin films; second part gives details about thermal chemical vapor deposition (TCVD) with CNT growth process, the following section is focused on characterization techniques which are SEM, TEM, and AFM.

4.1. DC Magnetron Sputtering Process

Many techniques have been used to grow thin film some of them chemical some of them are physical methods; in this thesis work, DC magnetron sputtering process which is a physical method was performed to deposit thin films. It has several advantages over the other conventional thin film deposition techniques, such as good surface uniformity, growth on substrates, and its cost effectiveness.

In this study, DC magnetron sputtering process was used to deposit Fe, Co catalyst thin films and Al₂O₃ support layer on the SiO₂/Si substrate. For this process, AJA ATC Orion 5 UHV sputtering system based in Magnetism Lab, IYTE was used to grow thin films.

In the basic sputtering process, a target (cathode) plate is bombarded by energetic ions generated in glow discharge plasma, situated in front of the target. The bombardment process causes the removal of target atoms, which may then condense on a substrate as a thin film (Kelly, et al. 2000). Secondary electrons are also emitted from the target surface as a result of the ion bombardment, and these electrons play an important role in maintaining the plasma (Kelly, et al. 2000). Magnetrons make use of the fact that a magnetic field configured parallel to the target surface can constrain

secondary electron motion to the vicinity of the target. The magnets are arranged in such a way that one pole is positioned at the central axis of the target and the second pole is formed by a ring of magnets around the outer edge of the target (Kelly, et al. 2000).



Figure 4.1. The TCVD system based in Physics Department, CNL Lab, IYTE

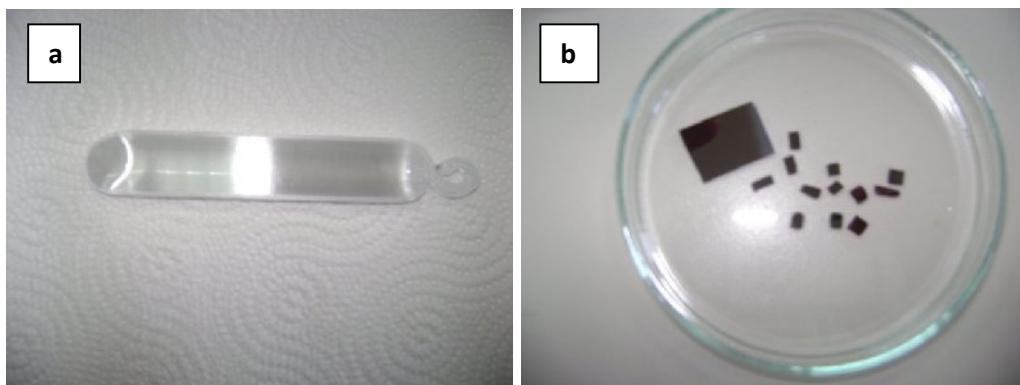


Figure 4.2. a) Quartz boat, b) Some thin films used for CNT growth

4.2. Thermal Chemical Vapor Deposition with CNT Growth Process

The TCVD method was used to grow CNT, the system has two dependent parts, upper part is a Lindberg/Blue M 1100 C0 Split Mini Furnace and the other dependent part is a controller. Figure 4.1 is showed the TCVD system. For this furnace quartz tube and quartz boat are used because of the experiments are performed at high temperature so the melting point of quartz is higher than the experiment temperature. The images of quartz boat and tube are shown in Figure 4.2 and Figure 4.1, respectively.

The location of samples and the quartz boat in the furnace is also so important, because there is an isothermal area in the middle of the furnace. The upper temperature limit of the furnace is 1100 °C however; the furnace should not be stable at the maximum limits of temperature. The maximum point in this study is 800 °C.

In this study, the experiment was performed at low vacuum (between 2.0 -4.5 Torr) until growth process to create vacuum area a rough pump is used, Ar gas sent into the system during all experiment to remove the contamination and to prevent the oxidation of the samples. Until the temperature reach the selective point, only Ar gas flows through the quartz tube and at the set point of temperature hydrogen gas is started to send with Ar gas during 15 minutes. The treatment time can be changed in some part of study to search as a parameter. Hydrogen gas is used as an echant gas. The flow rates of these gases are 150 sccm Ar gas and 140 sccm hydrogen gases. When the treatment time finishes, the rough pump is turned off and the pressure in the furnace starts to increase and when the furnace pressure reaches the atmospheric pressure the vane which is between the furnace and the glycerin cap is opened to perform the experiment at atmospheric pressure.

Growth time is also a parameter for CNTs, in this study the growth time is 15 minutes for all of the experiments. This parameter affects the length of CNTs not the growth mechanism so 15 minutes is enough for this study.

When the growth time is finished, first the hydrocarbon gas is turned off and then the hydrogen gas, Ar gas is stil flowing through the system and the temperature is fixed to 0 °C so the system is left for cooling under Ar ambient. All the growth conditions are listed in the Table 4.1.

Table 4.1. Growth conditions of CNTs for TCVD method

Sample Name	Temp. (°C)	Ar (sccm)	C ₂ H ₄ (sccm)	H ₂ (sccm)	P _{growth} (Torr)	P _{initial} (Torr)	Time (min)
FeAl05CNT238	730	150	120	140	750	2.8	15
FeAl08CNT245	750	150	120	140	750	3.0	15
FeAl06CNT254	750	150	180	140	750	3.0	15
FeAl08CNT256	750	150	180	140	750	3.0	15
FeAl09CNT257	750	150	180	140	750	3.0	15
FeAl10CNT258	750	150	180	140	750	3.0	15
FeAl06CNT261	750	150	150	140	750	3.5	15
FeAl08CNT263	750	150	150	140	750	3.5	15
FeAl09CNT264	750	150	150	140	750	3.5	15
FeAl10CNT265	750	150	150	140	750	3.5	15
FeAl08CNT276	750	150	210	140	750	2.9	15
FeAl09CNT277	750	150	210	140	750	2.9	15
FeAl10CNT278	750	150	210	140	750	2.9	15
FeAl10CNT332	750	150	210	140	750	2.4	15
FeAl06CNT333	750	150	210	140	750	2.4	15
CoAl01CNT334	750	150	180	140	750	2.2	15
FeAl08CNT338	700	150	180	140	750	2.3	15
CoAl01CNT339	700	150	180	140	750	2.3	15
FeAl08CNT347	650	150	180	140	750	2.3	15
CoAl01CNT348	650	150	180	140	750	2.3	15

4.3. Characterization Techniques

Characterization of CNTs is the most important part to discuss the results and this part is base for future work. Carbon nanotubes have very different structural properties and without characterization, nothing can be said for CNTs. In this study, SEM (Scanning Electron Microcopy), TEM (Transmission Electron Microscopy), AFM (Atomic Force Microscopy) were used.

4.3.1. Scanning Electron Microscopy

SEM (Scanning Electron Microscopy) is the most significant electron-optical method to investigate of bulk material especially, carbon nanotubes. For growing CNT, finding the suitable parameter is the long period and in this duration SEM is the first method to characterize the CNTs. SEM is used to measure the diameter of CNT roughly and to see the density of CNTs on the surface.

Electrons thermionically emitted from cathode filament to an anode, focused by two successive condenser lenses into a beam with a very fine spot size. Pairs of scanning coils located at the objective lens deflect the beam either linearly. Electrons beams having energies ranging from a few thousand to 50 keV, with 30 keV a common value are utilized. The most common imaging mode relies on detection of very lowest portion of the emitted energy distribution. The low energy means they originate from a subsurface depth of no longer than several angstroms. The signal is captured by a detector consisting of a scintillator-photomultiplier combination (O'Connor, et al.2003). The SEM utilized throughout this thesis work was Philips XL 30S, FEG.

4.3.2. Transmission Electron Spectroscopy

TEM is used to determine structural information from specimens that are thin enough to transmit electrons. A thin solid specimen is bombarded in vacuum with a highly focused, monoenergetic beam of electrons.

The beam is of sufficient energy to propagate through the specimen. A series of electromagnetic lenses then magnifies this transmitted electron signal. Diffracted electrons are observed in the form of a diffraction pattern beneath the specimen. This information is used to determine the atomic structure of the material (O'Connor, et al.2003).

4.3.3. Atomic Force Microscopy

Atomic Force Microscopy (AFM) is a mechanical imaging instrument which measures the three dimensions of sample. The advantages of this microscopy is analysing any type of surface, including ceramics, glass, polymers and biological samples. AFM relies on the atomic forces between the sample surface and the tip. To take good image from AFM scanning, the tip should be very sharp and it should be close enough to the surface. AFM consist of a sharp tip, a cantilever, piezoelectric scanner, photodiode, detector and feedback electronics.

According to applications, AFM can be performed in some modes such as; contact mode, tapping mode and non- contact mode. Generally tapping mode is used because of not damaging the sample surface, while in the contact mode, there is an interaction between the tip and the surface atoms and in this mode the surface of the material is scratched.

CHAPTER 5

RESULTS AND DISCUSSION

This chapter is focused on the results and discussions of the experiments. First section is about determining the parameters to grow vertical carbon nanotubes; the next part is about support layer effect on the CNT growth. The following section is devoted to compare the catalyst thin films which are Fe and Co catalysts; the following part examines hydrogen pretreatment time effect on the CNT growth, finally the last section is about the electrical properties of CNTs. For this discussion, AFM, SEM, TEM, the surface characterization techniques were used and also two-point contact method was used to determine the electrical characterization of CNTs.

5.1. SEM and AFM Results

5.1.1 Growth of Aligned Carbon Nanotubes

Carbon nanotubes have several advantages for practical applications. However, the preferable form of nanotubes for these applications is aligned, thin and long carbon nanotubes.

Several parameters are effective to growth vertical nanotubes such as, the type and thickness of support layers and catalyst thin films. Moreover, the hydrocarbon and etching gases and also the ratio between these gases, the other one is pretreatment time of etching gas, the last thing is experiment conditions, for example, temperature, pressure and also the growth time.

In this study, all parameters which is mentioned in above paragraph, have tried to grow vertical nanotubes. Nearly, three hundreds experiments have done to see the best result. Firstly, the hydrocarbon gas was changed, ethylene was used instead of

methane gas and second step was adding SiO₂ buffer layer to Al₂O₃ buffer layer and the results were better than the previous samples but not exactly the best results. Three different thicknesses of Al₂O₃ thin films were used and the final step is the pretreatment time. For some experiments, the pretreatment process was not applied and sometimes, the etching gas, hydrogen, was sent the system after a few minutes than the hydrocarbon gas. The result still was not perfect, finally pretreatment time was performed 15 minutes and then the ethylene gas was sent the system and the conclusion was perfect. The following SEM images show the steps of growing vertical nanotubes.

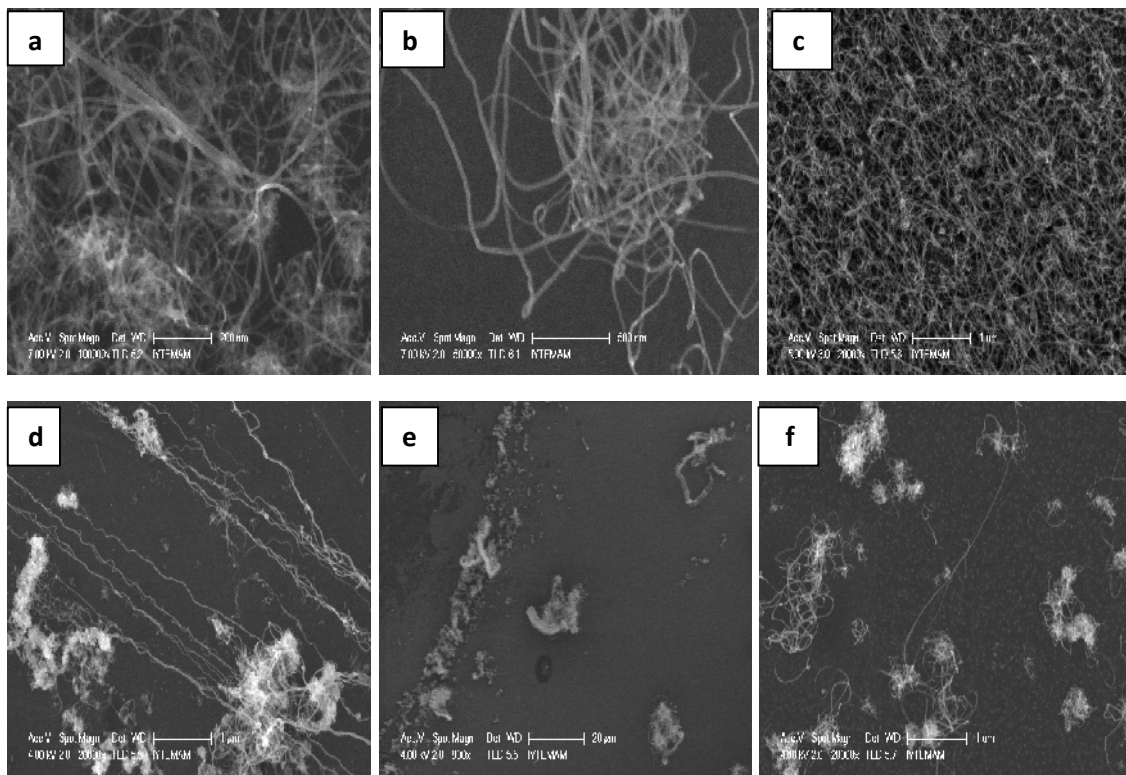


Figure 5.1. SEM micrographs of a) FeAl10CNT258 b) FeAl06CNT254 c) FeAl08CNT245 d) FeAl05CNT238 e) FeAlCNT232 f) FeAl06CNT235

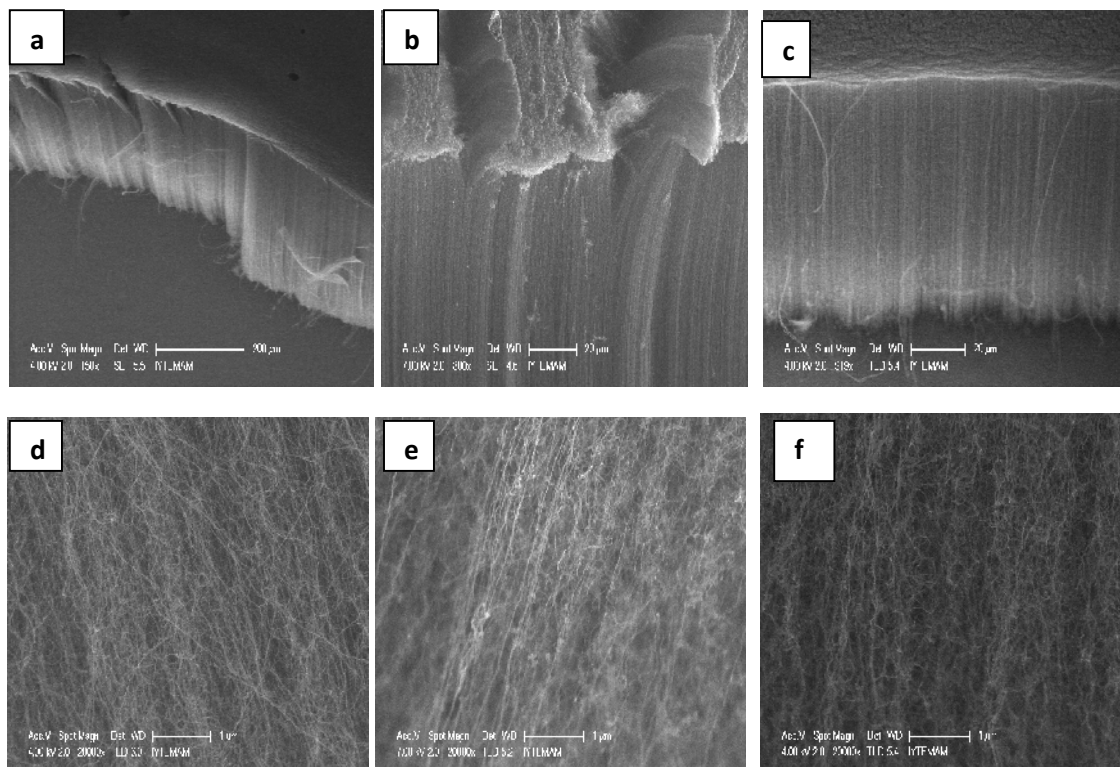


Figure 5.2. SEM micrographs of a) FeAl08CNT256 b) FeAl08CNT256 c) FeAl09CNT257 d) FeAl09CNT257 e) FeAl08CNT263 f) FeAl08CNT263

All images in Figure 5.2 are called carbon nanotubes forest and this forest can be easily removed from substrate, for example, by a razor. After removing CNTs, the same sample was used again and also CNTs were produced as before. It means catalyst nanoparticles were on the surface and CNTs were purity because they did not contain any catalyst particles. The lengths of CNTs are nearly 200 μm . The vertical and denser carbon nanotubes were grown on Si/ SiO_2 / Al_2O_3 /Fe samples because Fe has much less mobility on Al_2O_3 with respect to SiO_2 (Mattavi, et al. 2008). The table 5.1 gives the experiment conditions of samples in Figure 5.1 and in Figure 5.2.

Table 5.1. Growth parameters of some steps to have vertical CNTs

Sample	Temp. (°C)	SiO ₂ (nm)	Al ₂ O ₃ (nm)	Treat.Time (min.)	Catalyst	C ₂ H ₄ /H ₂
FeAl07CNT232	730	0	30	0	Fe	120/140
FeAl06CNT235	730	0	30	0	Fe	120/140
FEAl05CNT238	730	0	30	2	Fe	120/140
FeAl08CNT245	750	1000	15	0	Fe	120/140
FeAl06CNT254	750	0	30	15	Fe	180/140
FeAl08CNT256	750	1000	15	15	Fe	180/140
FeAl09CNT257	750	1000	20	15	Fe	180/140
FeAl10CNT258	750	1000	30	15	Fe	180/140
FeAl08CNT263	750	1000	15	15	Fe	150/140

5.1.2. Support Layer Effect on the CNT Growth

In this part, CNT growth was applied on two different types of sample to investigate the effect of support layer and also the thickness of support layer; the first one was Si/Al₂O₃ /Fe (thickness of layers are 30 nm, 1.5 nm, respectively) and the second one was Si/SiO₂/Al₂O₃/Fe (thickness of layer are 1000 nm and 30 nm, 1.5 nm, respectively). The second sample did not include SiO₂. All the experiments for this part were performed at 750⁰C, with different hydrocarbon and hydrogen gas ratio datas which were 150/140, 180/140, 210/140. First two samples, FeAl06CNT 261, FeAl10CNT 265, were performed at 150/140.

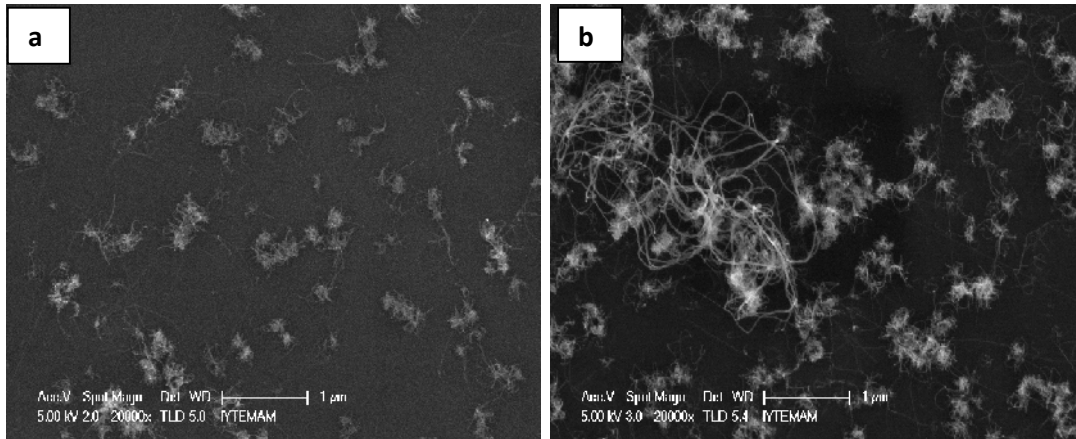


Figure 5.3. SEM micrographs of, a) FeAl106CNT261 b) FeAl110CNT 265 with the 150/140 C_2H_4/H_2 ratio

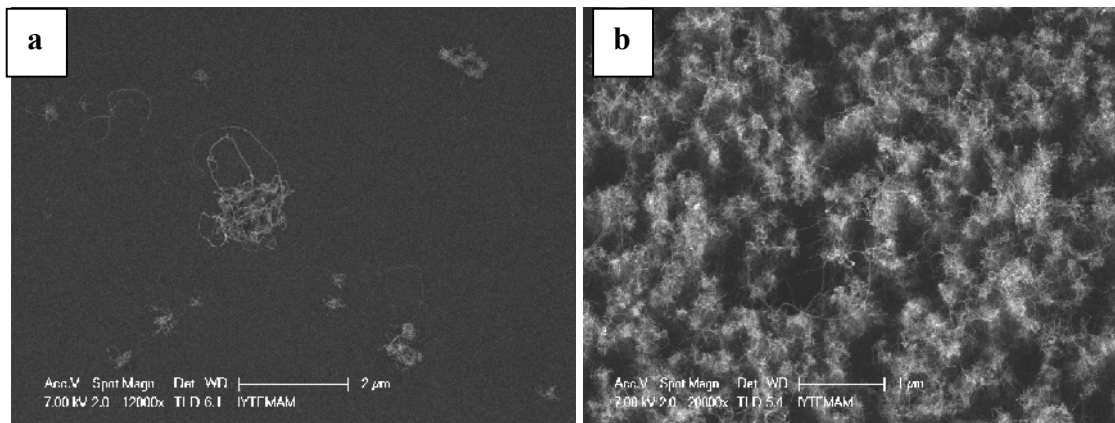


Figure 5.4. SEM micrographs of, a) FeAl106CNT 254 b) FeAl110CNT 258 with the 180/140 C_2H_4/H_2 ratio

It is clearly seen in Figure 5.4 that the density of carbon nanotubes sharply increases when SiO_2 is used as a buffer layer with Al_2O_3 . Carbon nanotubes are in small bundle shape and there are only a few nanotubes on the surface of FeAl106CNT 254.

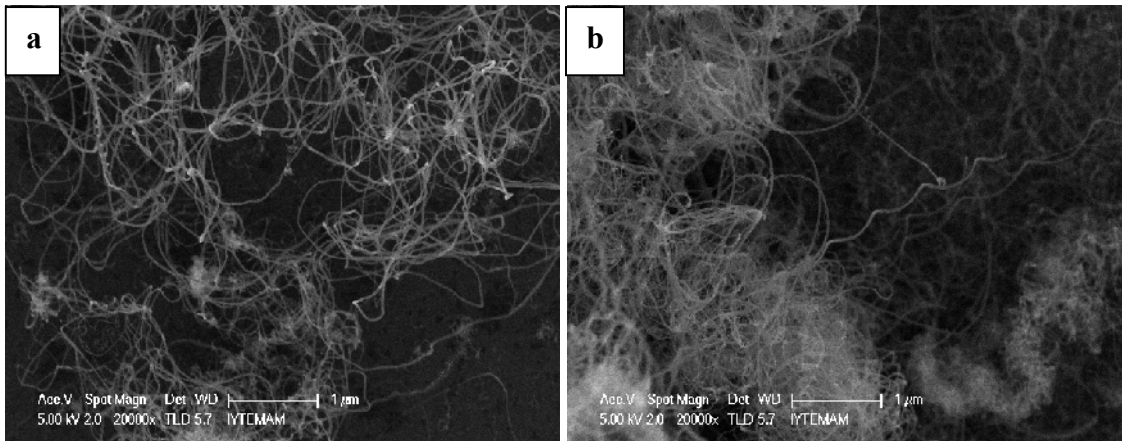


Figure 5.5. SEM micrographs of, a) FeAl106CNT 333 b) FeAl110CNT 332 with the 210/140 C_2H_4/H_2 ratio

In three images which include the extra SiO_2 support layer, have denser carbon nanotube density. Because samples FeAl106CNT 261, FeAl106CNT 254, FeAl106CNT 333 have only 30 nm Al_2O_3 as a buffer layer and this thickness is not enough to prevent forming metal silicide between Si and the catalyst metal particles (Arcos, et al. 2002, Teo, et al. 2002). Al_2O_3 is an effective support material because it is a porous material and this feature is important to grow vertical carbon nanotubes. However, it is clearly seen that only thin Al_2O_3 is not suitable for CNTs when SiO_2 whose thickness was 1000 nm was used with Al_2O_3 double buffer layer, it gave the better results.

5.1.3. Catalyst Thin Film Effect on the CNT Growth

In growing CNT process, one of the most important parts is catalyst materials. Because catalyst affect directly the size and the density of CNTs and also the types of this catalyst is so important because only some elements are suitable to use as catalyst and the relation between the catalyst and hydrocarbon gas is so important, too. In this part Si/ SiO_2 / Al_2O_3 / Fe and Si/ SiO_2 / Al_2O_3 / Co thin films were used as sample and Co and Fe are the catalyst thin films. The thickness of sample parts are the same, 1000 nm SiO_2 , 30 nm Al_2O_3 and 1.5 nm Fe or Co thin films. At three different temperatures, 650 °C, 700 °C and 750 °C, the experiments were performed. The following SEM images give information about Co and Fe catalyts.

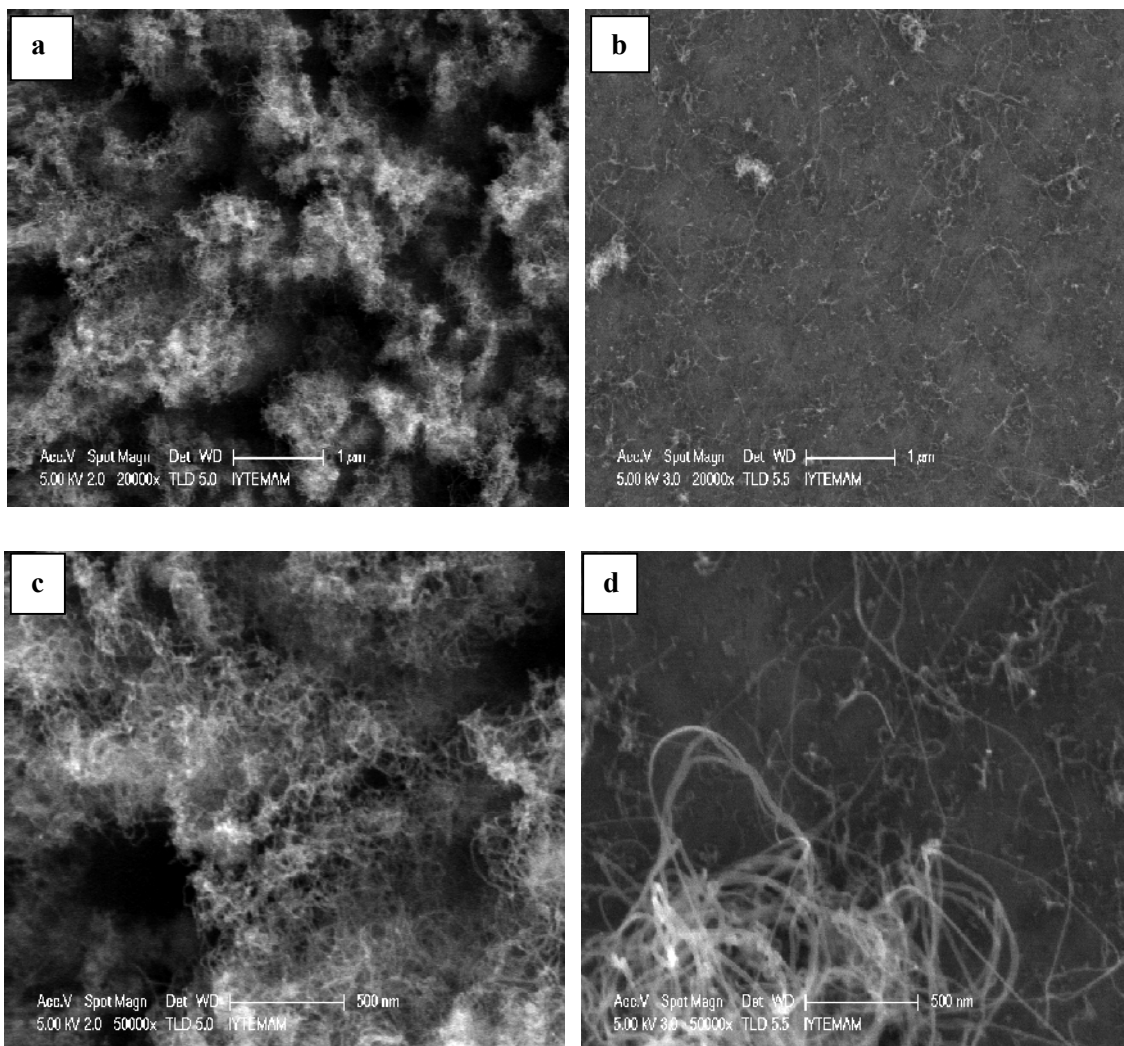


Figure 5.6. SEM micrographs of, a) FeAl08CNT 319 b) FeAl08CNT 319 c) CoAl01CNT 334 d) CoAl01CNT 334 at 750 0C with 20000X and 50000X magnification.

The above samples, FeAl08CNT 319 and CoAl01CNT 334 were performed at 750 °C. The average diameters of FeAl08CNT 319 and CoAl01CNT334 are nearly 10 nm and 20 nm, respectively. Also it is seen in images the carbon nanotubes on Fe catalyst thin film are denser like a nanotube cloud however, the tubes are scarce on Co catalyst film.

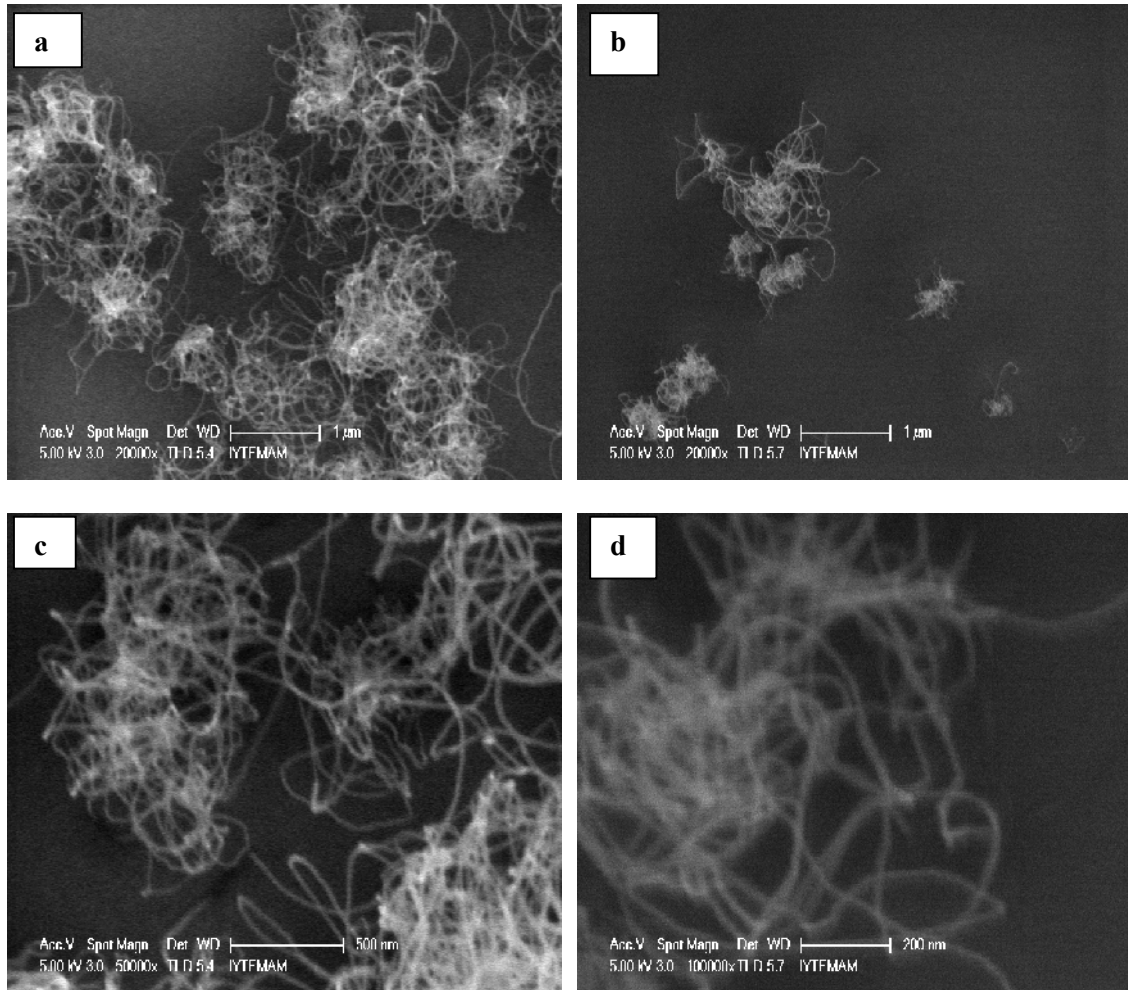


Figure 5.7. SEM micrographs of, a) FeAl08CNT 356 b) FeAl08CNT 356 c) CoAl01CNT 355 d) CoAl01CNT 355 at 700 °C with 20000X and 50000X magnification.

FeAl08CNT 356 and CoAl01CNT 355 were performed at 700 °C and when temperature was decreased from 750 °C to 700 °C, the density of CNTs was decreased on both Fe and Co catalyst thin films. However, CNTs are still denser on Fe catalyst; there are only a few bundle of CNT on Co film. This means that there are only a few Co catalyst particles. It can be followed from AFM images for this sample. Also the average diameters of FeAl08CNT 356 and CoAl01CNT 355 are 15 nm and 28 nm, respectively.

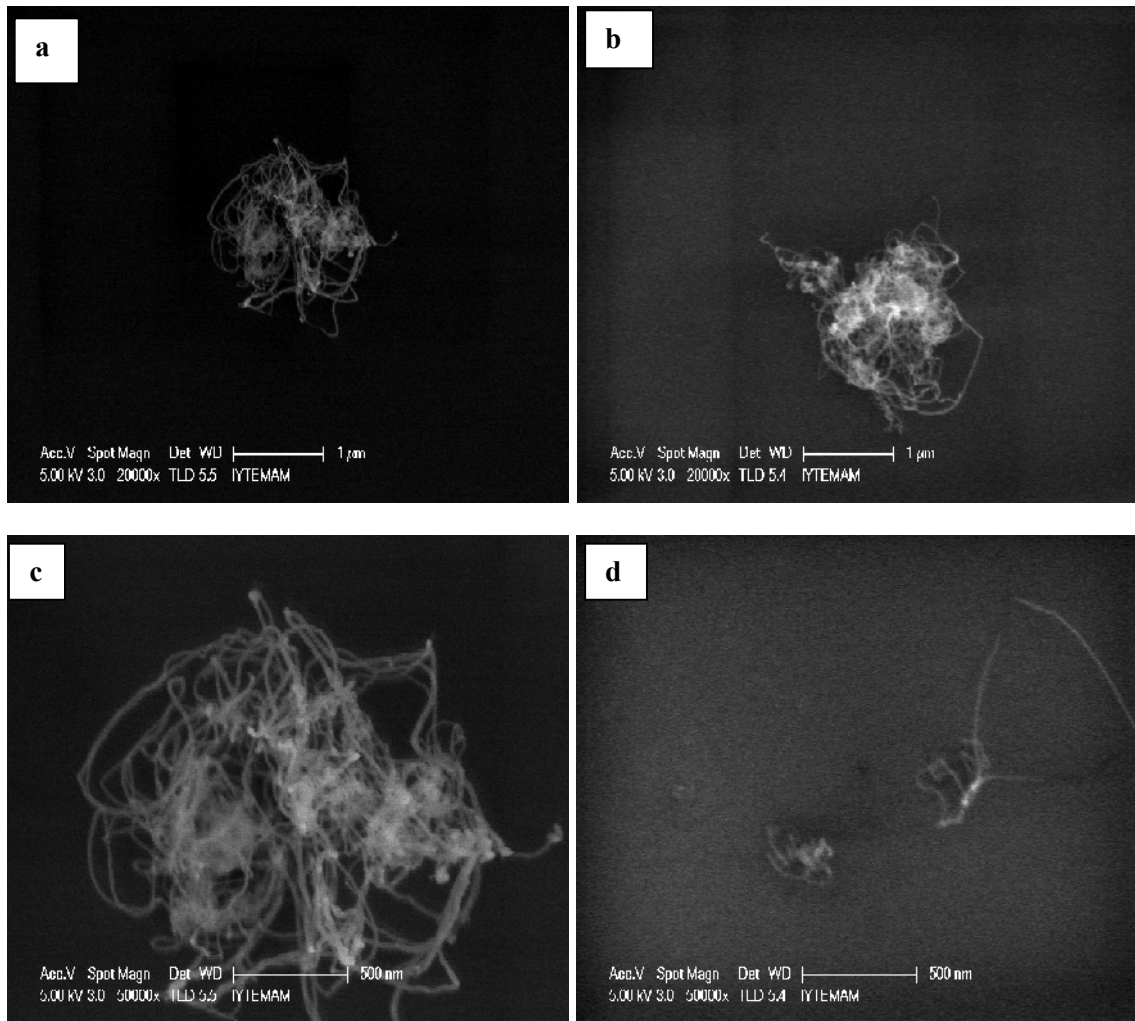


Figure 5.8. SEM micrographs of, a) FeAl08CNT 347 b) FeAl08CNT 347 c) CoAl01CNT 348 d) CoAl01CNT 348 at 650 °C with 20000X and 50000X magnification.

The temperature was decreased 50 °C and the experiment was performed at 650 °C and it is clearly seen that the growth of CNT sharply decreased both on Fe and Co catalyst films. This temperature was not enough for reaction for hydrocarbon and hydrogen gases to occur carbon nanotubes. CNTs are in bundle form; however the diameter of FeAl08CNT 347 and CoAl01CNT 348 can be measured roughly, as 25 nm and 35 nm, respectively.

Table 5.2. Growth parameters of CNTs on Fe and Co catalyst thin films

Sample	Temp. (°C)	Thick. catalyst (nm)	C ₂ H ₄ /H ₂	Average diameter (nm)	P _{growth} (Torr)
FeAl08CNT 347	650	1.5	180/140	~ 25	750
CoAl01CNT348	650	1.5	180/140	~ 35	750
FeAl08CNT 356	700	1.5	180/140	~ 15	750
CoAl01CNT355	700	1.5	180/140	~ 28	750
FeAl08CNT 319	750	1.5	180/140	~ 10	750
CoAl01CNT334	750	1.5	180/140	~ 20	750

The diameters of CNTs are directly related to the diameters of catalyst nanoparticles. The resolution of SEM was not enough to measure the diameters of catalyst nanoparticle so AFM (Atomic Force Microscopy) was used to determine the catalyst particles and roughly their diameters were measured. The following table shows the diameters of catalyst nanoparticles.

Table 5.3. Growth parameters of Fe and Co catalyst nano particles

Sample	Temp.(°C)	Averag. diamtr (nm)	C ₂ H ₄ /H ₂
FeAl08 357	650	~ 67	180/140
CoAl01 358	650	~ 85	180/140
FeAl08 362	700	~ 45	180/140
CoAl01 363	700	~ 75	180/140
FeAl08 322	750	~ 25	180/140
CoAl01 364	750	~ 53	180/140

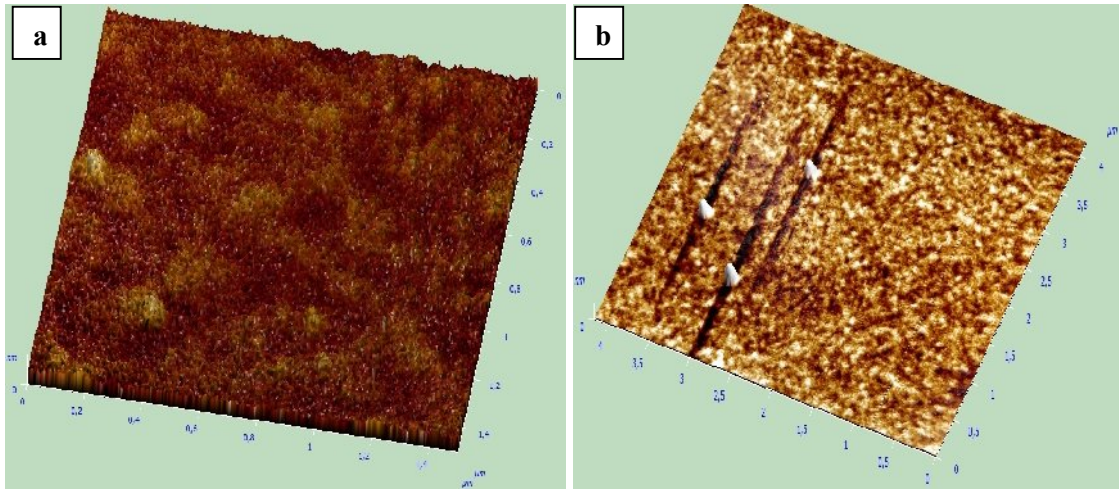


Figure 5.9. AFM micrographs of, a) FeAl08 357 b) CoAl01 358 at 650 °C

The above AFM images give information for catalyst nanoparticles, at 650 °C Fe nanoparticles were not exactly occurred, the lighter parts on Fe surface show the catalyst particles and they do not have a smooth shape; however Fe catalyst particles are on the full of surface not only some parts. Unlike Fe particles, the number of Co particles is only a few. There are only three big catalyst particles are seen Co catalyst film surface. In SEM images at above a few nanotubes in bundle form can be seen at 650 °C so the catalyst images proved this reason because there are only a few catalyst particles. This result shows to have nice tubes, growing nice form of catalysts.

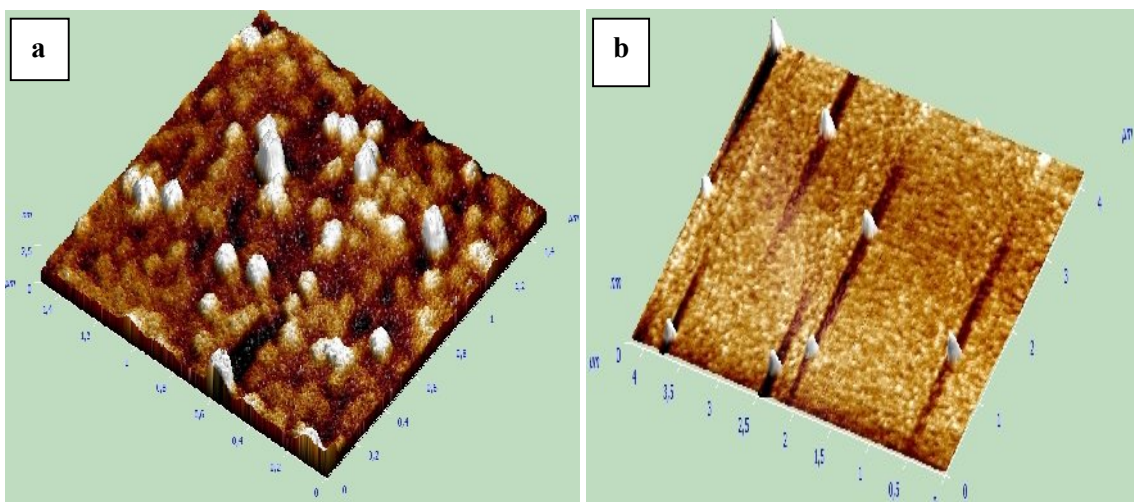


Figure 5.10. AFM micrographs of, a) FeAl08 362 b) CoAl01 363 at 700 °C

When the temperature was increased 50 °C, the uniformity, density and the clarity of Fe catalyst particles were increased which can be seen in above figure. The brighter parts show the higher particles. The number of Co particles showed a small increasing. In SEM images there are only a few CNT bundle at 700 °C. The average diameters of catalyst particles are 45 nm and 75 nm. Scanning area of samples are 1.5 X 1.5 μm² for Fe and 4.5 X 4.5 μm² and Co thin films.

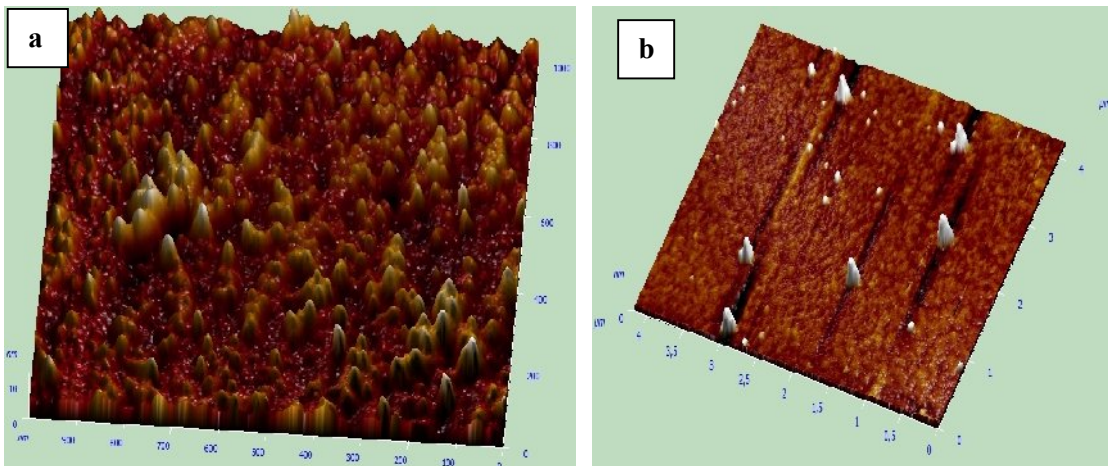


Figure 5.11. AFM micrographs of a) FeAl08 322 b) CoAl01 364 at 750 °C

The difference of effectivity increased when the temperature was increased again 50 °C. It is clearly seen in Figure 5.11 Fe catalyst particles gave better results than Co particles at 750 °C with ethylene gas. The numbers of catalyst particles increased; however the diameters of particles decreased by increasing temperature. Both AFM and SEM images showed the densest samples were Fe catalyst and Co was not effective with ethylene gas.

5.1.4. H₂ Pretreatment Time Effect on CNT Growth

In the mid 1970s, the importance of atomic hydrogen in the CVD growth of diamond was recognized. The crucial role of hydrogen is to etch away graphitic structures and allow both high nucleation density and practical growth rates (Jean

Bonard 2006). Hydrogen is a significant element to change the surface morphology of the catalyst (Baker, et al.1982). Hydrogen treatment is also a parameter for CNT growth and it is a time dependent process.

During this study it was understood that hydrogen pretreatment was an important parameter for this experiment conditions. So in this part of study, H₂ treatment was researched for seven different time durations which were 0, 5, 10, 15, 20, 25 and 30 minutes before sending hydrocarbon gas through the system at growth temperature. SEM was not enough to analyse the particles so AFM was used to determine the diameters and densities of the catalyst nanoparticles. The following table shows the growth parameter of catalyst nanoparticles.

Table 5.4. Growth conditions of catalyst particles for TCVD method

Sample Name	T (°C)	Ar (sccm)	C ₂ H ₄ /H ₂ (sccm)	Averag. diamtr (nm)	P _{growth} (Torr)	P _{initial} (Torr)	Pretreat. Time (min)
FeAl08 303	750	150	-/140	~ 40	750	2.8	10
FeAl08 306	750	150	-/140	~ 50	750	2.5	5
FeAl08 313	750	150	-/140	~ 48	750	3.0	25
FeAl08 316	750	150	-/140	~ 58	750	3.0	0
FeAl08 322	750	150	-/140	~25	750	3.0	15
FeAl08 326	750	150	-/140	~ 32	750	2.7	20
FeAl08 329	750	150	-/140	~ 60	750	2.7	30

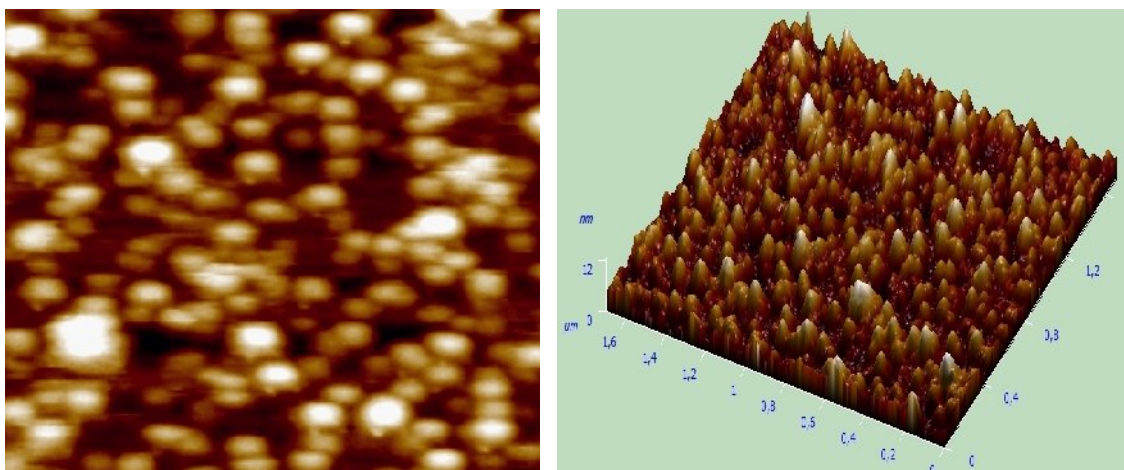


Figure 5.12. AFM micrographs of a) FeAl08316 b) FeAl08316 0 min. Treatment time

For 0 minute parameter, the catalyst particles can be seen in above AFM images. Only for this samples the scanning area of was $1.7 \times 1.7 \mu\text{m}^2$. The vertical CNTs did not occur at this parameter because the particles were not dense enough. When CNTs so close, they apply Van der Waals force to each other so it becomes easy to be align.

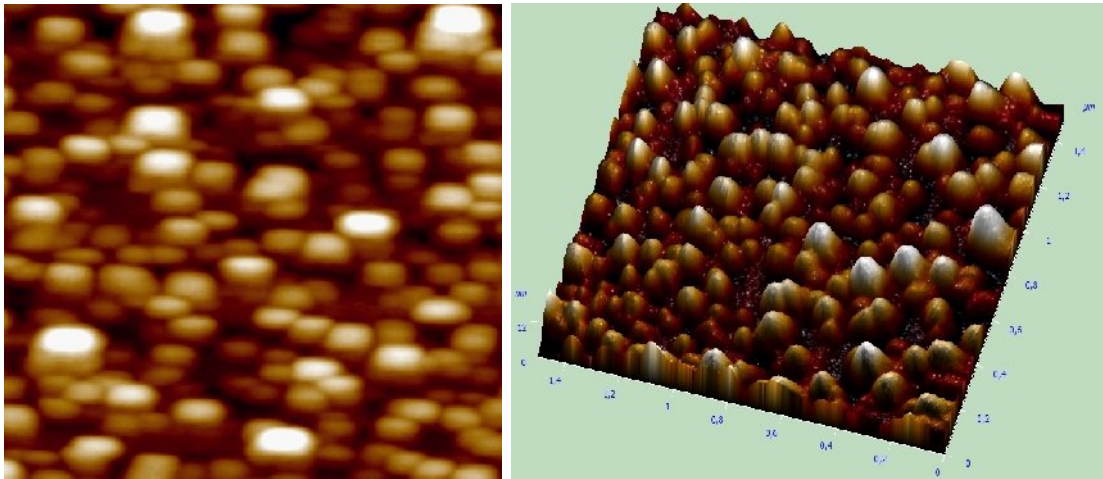


Figure 5.13. AFM micrographs of a) FeAl08306 b) FeAl08306 5 min. Treatment time

When the treatment time was increased 5 minutes, the catalyst number increased and they became closer and their diameters decreased from 58 nm to 50 nm. In 3-D image, the orientation of catalyst can be seen clearly. The scanning area is $1.5 \times 1.5 \mu\text{m}^2$.

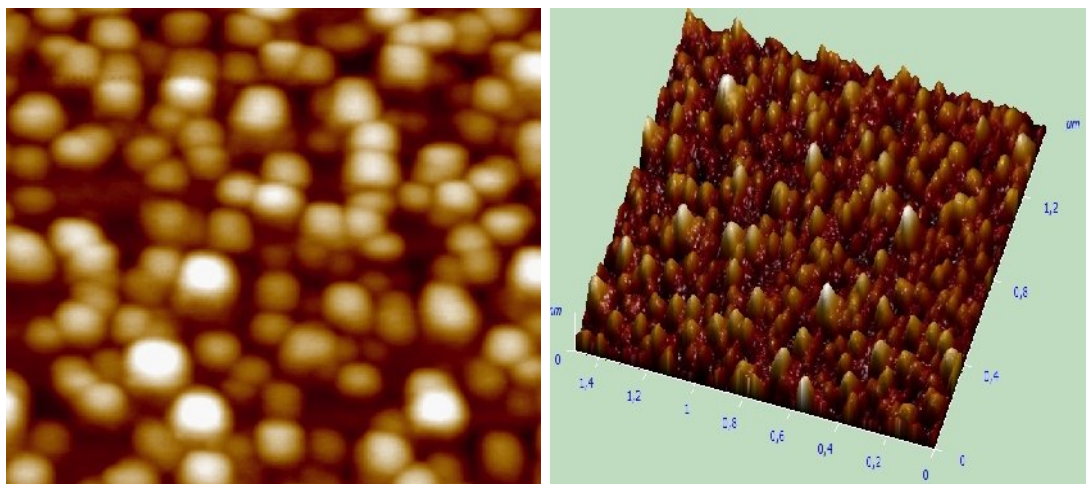


Figure 5.14. AFM micrographs of a) FeAl08303 b) FeAl08303 10 min. Treatment time

After increasing treatment time more 5 minutes, the density of catalyst was increased on the surface, too. Moreover the reducing of catalyst diameters continued, it decreased from 50 nm to 40 nm. Also the scanning areas are $1.5 \times 1.5 \mu\text{m}^2$ for this sample.

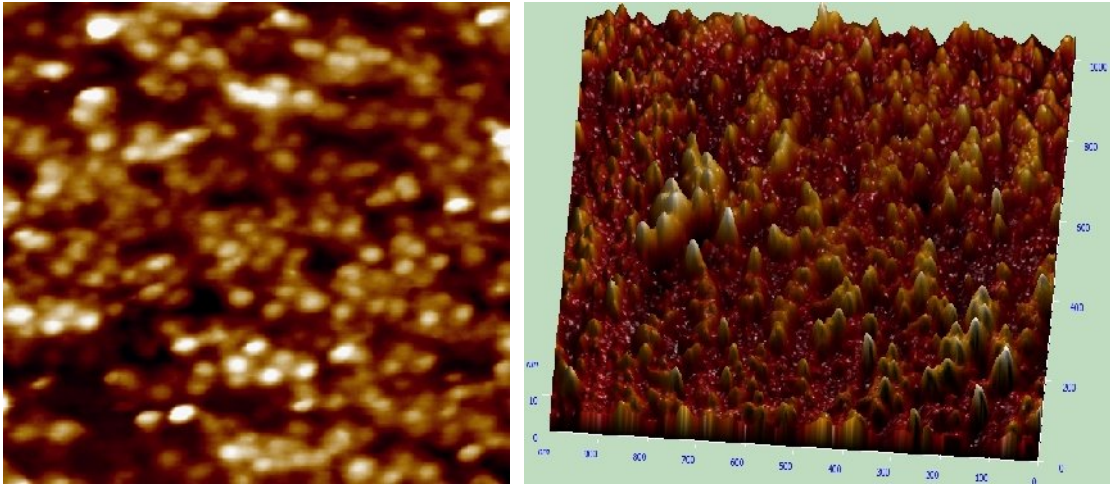


Figure 5.15. AFM micrographs of a) FeAl08322 b) FeAl08322 15 min. Treatment time

The scanning area of was $1.0 \times 1.0 \mu\text{m}^2$ for the above sample and this parameter gave the best result in this study. At this parameter, vertical carbon nanotubes could be grown. In Fig. 5.14-a, it can be seen that catalyst particles are so small according to previous images. Moreover, the scanning area was kept smaller to see the particles clearly. The average diameters of catalyst particles are 25 nm.

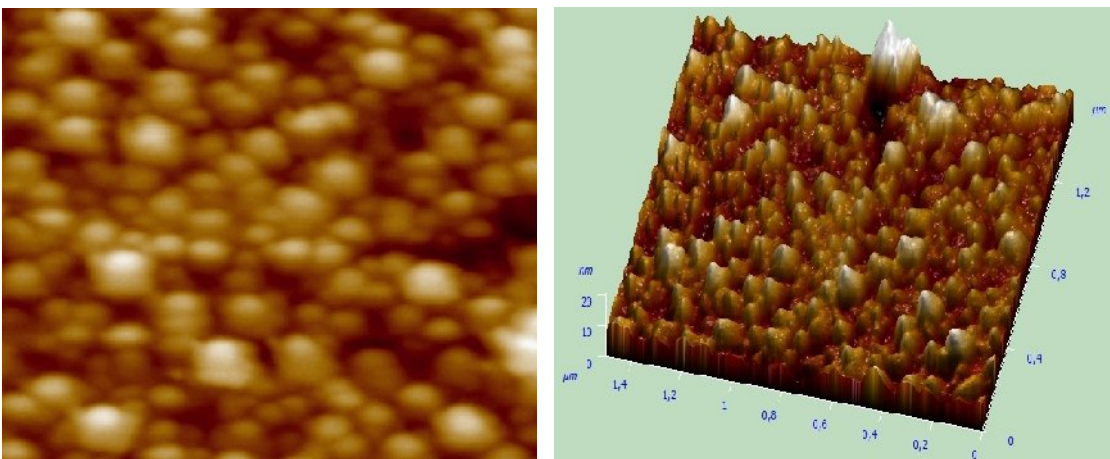


Figure 5.16. AFM micrographs of a) FeAl08326 b) FeAl08326 20 min. Treatment time

The pretreatment was again increased 5 minutes and it became 20 minutes, the above AFM images shows the catalyst particles are so dense on the surface and there are only a few particles which are bigger than the others. The diameters and the density is nearly the same after 15 and 20 minutes treatments.

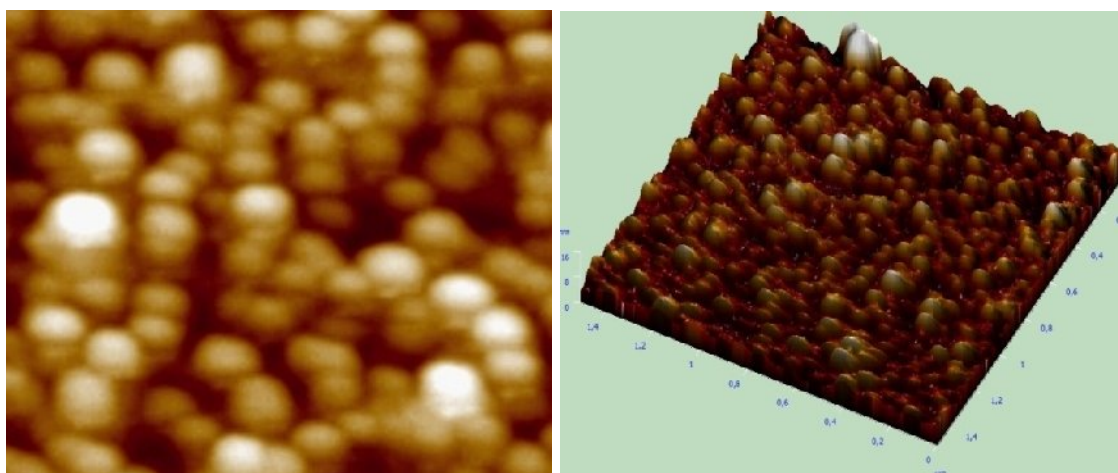


Figure 5.17. AFM micrographs of a) FeAl08313 b) FeAl08313 25 min. Treatment time

After 25 minutes treatments, the results showed that catalyst particles started to agglomerate. Hence, the catalyst diameters increased from 22 nm to 48 nm. The catalyst particles are not solid or liquid in that temperature and also they can migrate on the surface. However, oxygen atoms hold on to hydrogen atoms and after long hydrogen treatment the oxygen atoms are removed from the surface so Fe particles can easily move on the surface and they come together so, it increases the diameter of particles.

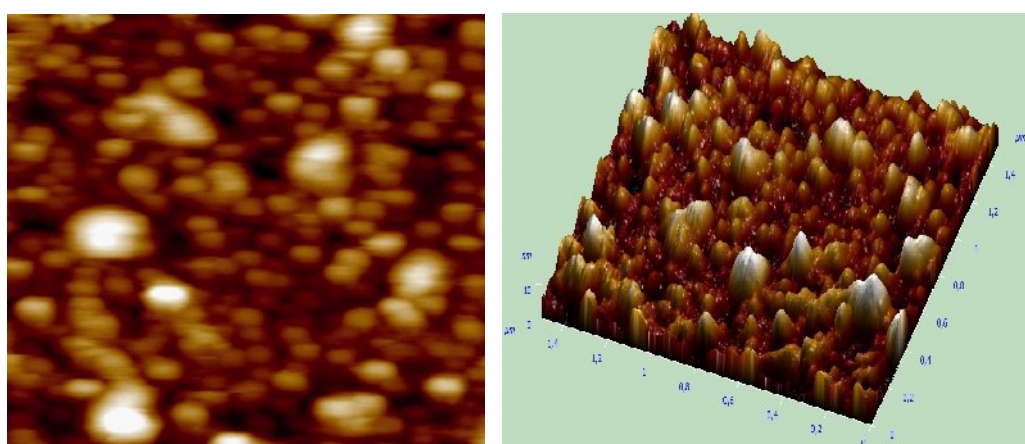


Figure 5.18. AFM micrographs of a) FeAl08329 b) FeAl08329 30 min. Treatment time

It is clearly seen in the above AFM images, the agglomeration of catalyst particles on the surface. The average diameters of catalyst were 48 for 25 minutes treatment and because of agglomeration the diameters again increased to 60 nm.

Finally, AFM images show that after a long period of H₂ pretreatment, nanoparticles tend to agglomerate to reduce surface energy. The small particles have higher surface energy than bigger particles. Initially, the particles decrease in size before agglomerating into a large one. When the duration time is long, the oxides are removed from surface so the catalyst particles tend to melt and agglomerate at high temperature.

5.2. TEM Results

TEM (Transmission electron microscopy) is one of the most important techniques to characterize carbon nanotubes and also it proves that CNTs can be occurred or not. TEM is used to determine the cristanility of CNTs. Sample preparation is so important for this method. In this study, samples were examined to see CNTs by TEM, in UNAM in Bilkent University.

Sample preparation has a significant position for this analysis method. For the samples which are mentioned in following table, some different method was used. Samples were put in a %99.9 ethanol solution and they were exposed to ultrasonic vibration because the CNTs had to solve in ethanol solution to analyse by TEM. However, a carbon film was coated on tubes and it prevented to see the nanotubes clearly. Because of ultrasonic vibration, vertical nanotubes became a bundle and they were damaged, too. It was decided to applied different method, again the sample were put in ethanol solution but were not exposed to ultrasonic, the solution was rank by human hand and a drop was taken and was put on a grid so the CNTs can be seen clearly. The other method was, the sample was sunk into liquid nitrogen a few minutes and the CNTs were inscribed by a tweezer and again the result was better than the other techniques. The lengths of CNTs were nearly 200 μm so, it was difficult to see CNTs with their walls because of vibration. The tubes were in vacuum and when they did not connect with grid line, it made high vibration. Because of this vibration problem, the wall number of some samples was not seen clearly. The following table gives information about the samples which was investigated by TEM.

Table 5.5. Parameters of CNTs which have TEM results

Sample	Temp.(C)	Inner dia. (nm)	Outer dia.(nm)	C ₂ H ₄ /H ₂ sccm	Ar sccm
FEAl08CNT256	750	10.5	13.8	180/140	150
FEAl09CNT264	750	10.7	16.8	150/140	150
FeAl10CNT269	750	8	11	150/140	150
FEAl08CNT273	750	5.5	9.8	180/140	200
FEAl09CNT277	750	8.5	12.1	210/140	150
FEAl08CNT296	750	6	9	180/90	150

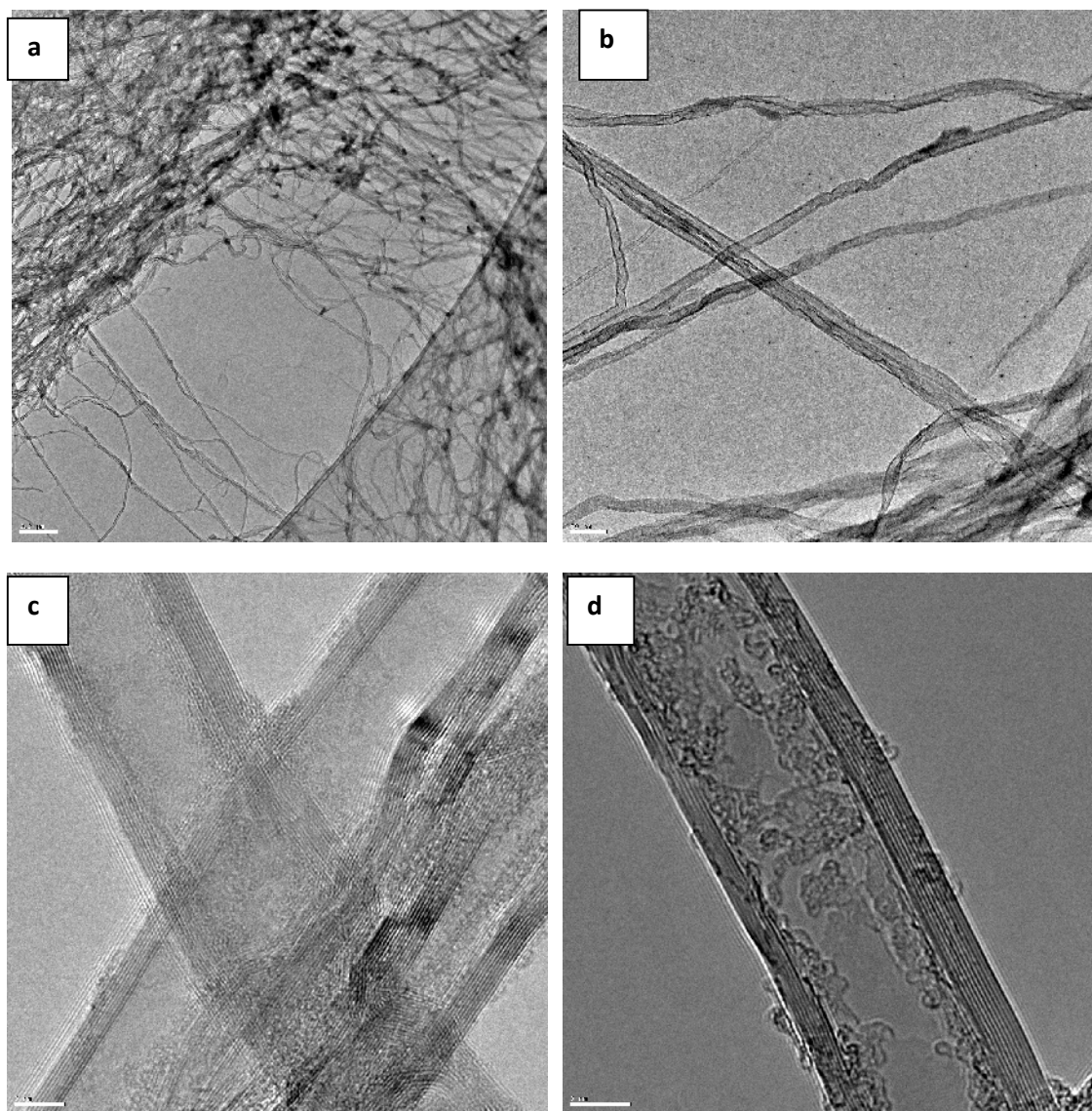


Figure 5.19. TEM micrographs of FeAl09CNT264 with four different magnifications

The nanotubes are clearly seen in above TEM images. The tubes crossed each other because of ultrasonic vibrations. The inner and outer diameters of this sample nearly are 8 nm and 11 nm, respectively. The number of walls are 11 and there are also some lines like walls but they occurred by vibrations of tubes .

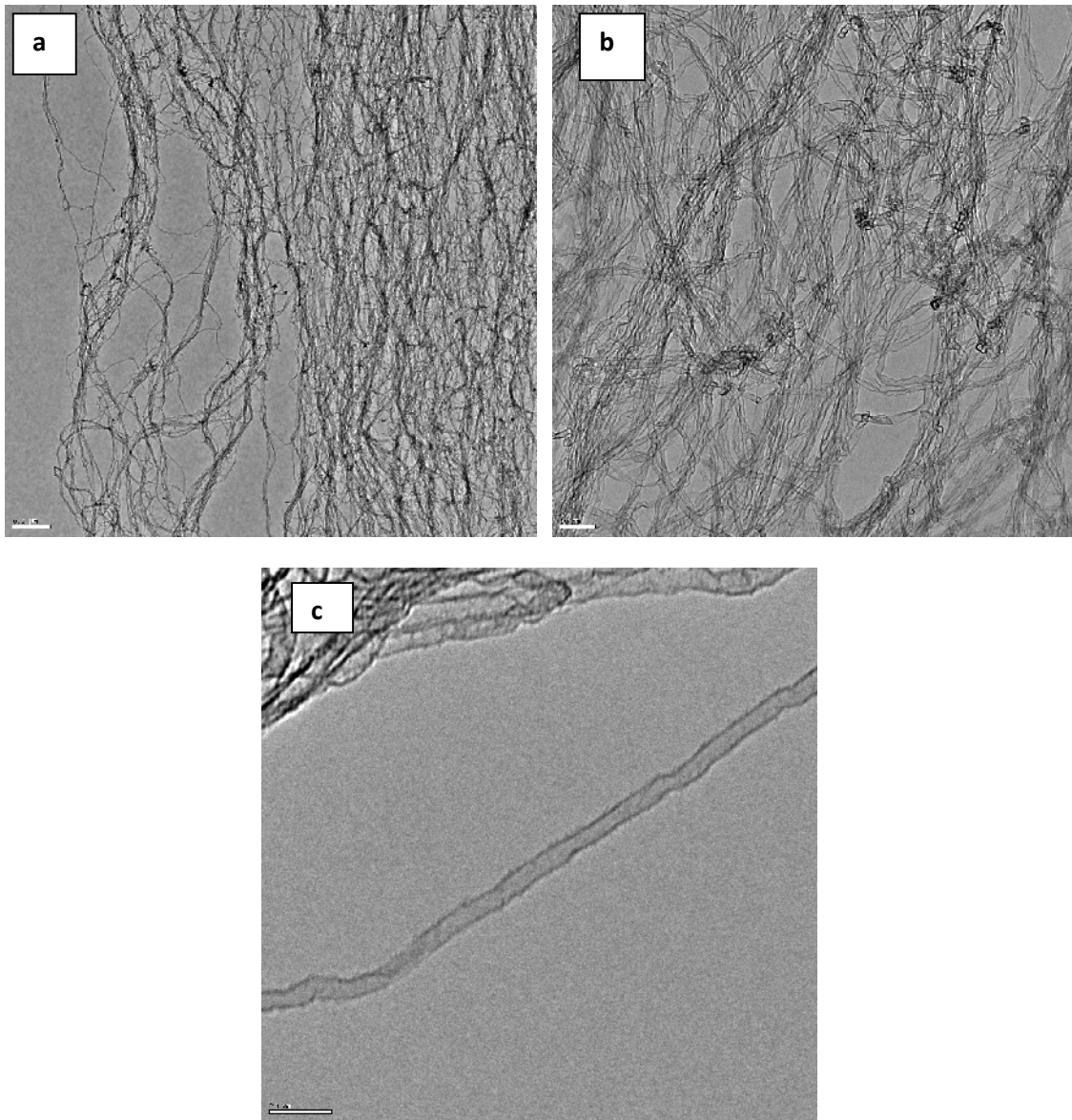


Figure 5.20. Three TEM micrographs of FeAlO8CNT296 with different magnifications

Aligned tubes can be seen in above TEM images; however there is no so closer image for this sample because of vibration, there is nothing to keep CNTs stable so

there is no information about the wall number of these CNTs. Nearly, the outer and inner diameters of samples are 9 nm and 6 nm, respectively.

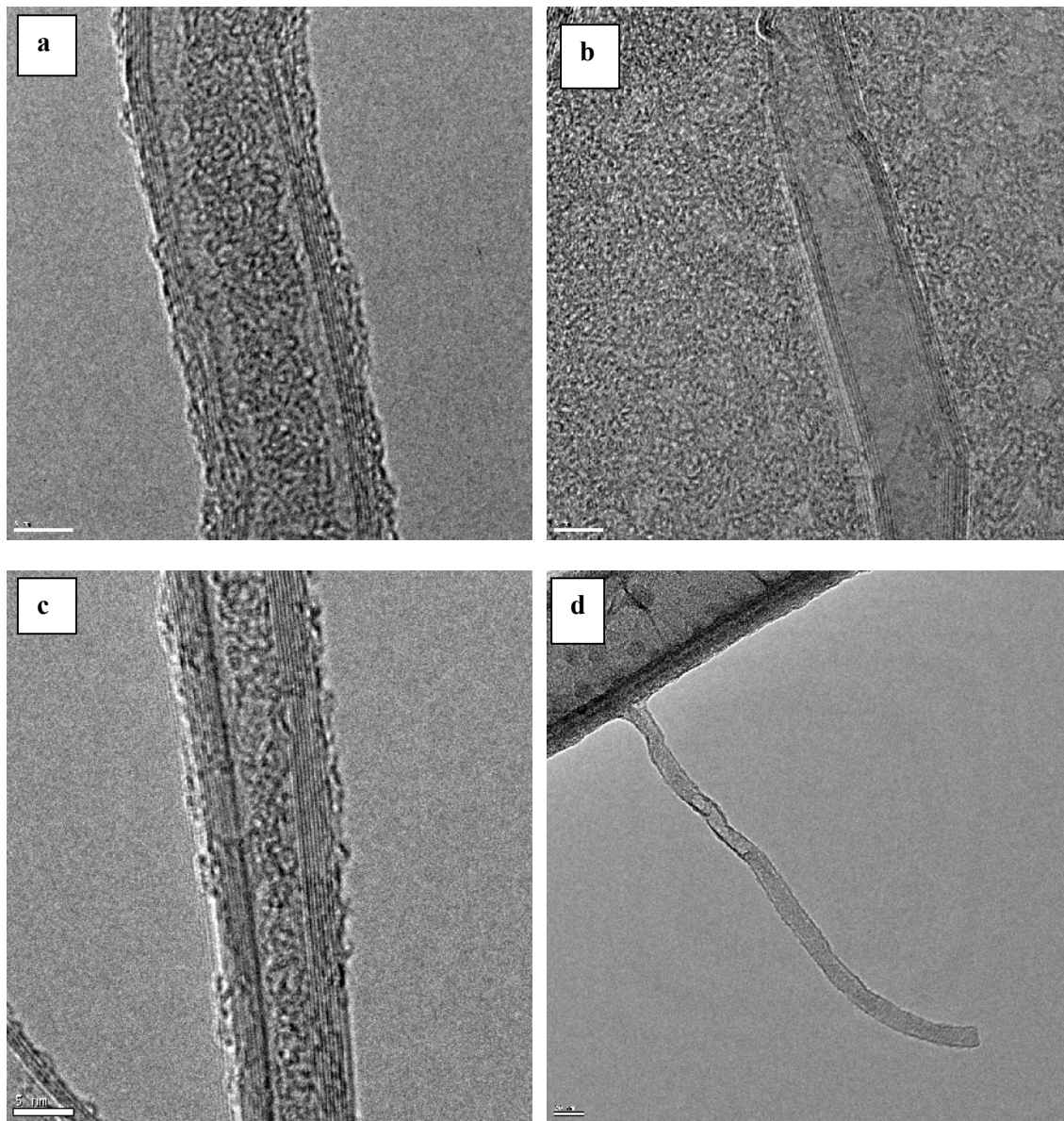


Figure 5.21. TEM micrographs of, a) FeAl08CNT 256 b) FeAl10CNT 269 c) FeAl08CNT 273 d) FeAl09CNT 277

The four samples have different wall numbers, inner and outer diameters. The first sample, FeAl08CNT 256, has 6 walls; the inner and outer diameters are 10.5 nm and 13.8 nm, respectively. The second sample is FeAl10CNT 269 with 4 wall numbers. The inner and outer diameters are 8 nm and 11 nm, respectively. The following one is

FeAl08CNT 273 which has 7 walls and it has 5.5 nm inner diameter and 9.8 nm outer diameters. The last one is FeAl09CNT 277. This sample has 8.5 nm inner diameter and 12.1 nm outer diameters, nearly. For this sample, it is difficult to say something about wall numbers because of there is no closer images for CNTs. TEM images show all the carbon nanotubes are multiwall carbon nanotubes and it has been known that all multiwall nanotubes are metallic .

5.3. Electrical Measurement Results

Although graphene is a zero-gap semiconductor, CNTs can be semiconductors or metals with different size energy gaps (Dresselhaus, et al. 2004). The types of CNTs can give some information about their electrical properties. There are some techniques to determine the electrical properties of CNTs. Four point and two point contact techniques, STM or Raman Spectroscopy can be used to characterize the CNTs.

In this study, two point contact method was used. The vertical CNTs were diluted in pure ethanol and small quartz was coated with this CNT solution and a gold electrode was coated by thermal evaporation system on this quartz. And then, contacts were made at the end points of gold electrode. The following step was receiving data for determine the resistance of CNTs. While taking data, a humidity sensor was used because the reaction of tubes with humidity was researched. The results of this investigation will show that CNT can be used as a humidity sensor or not. It is known that the conductivity is increased with increasing humidity. Also, the humidity source was K_2SO_4 solution with % 94 humidity ratio.

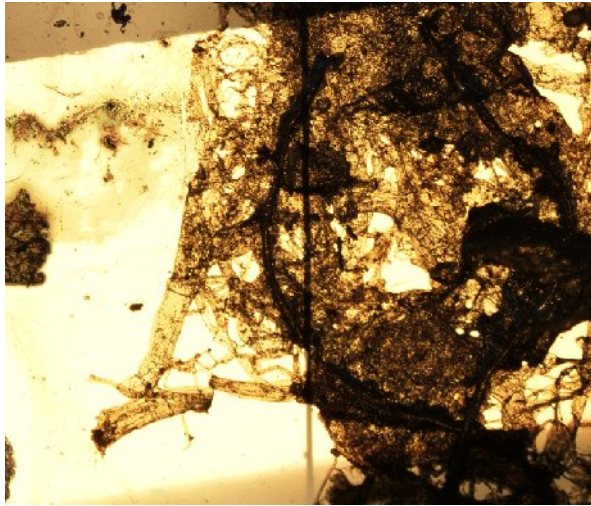


Figure 5.22. Photo of gold electrode with CNTs

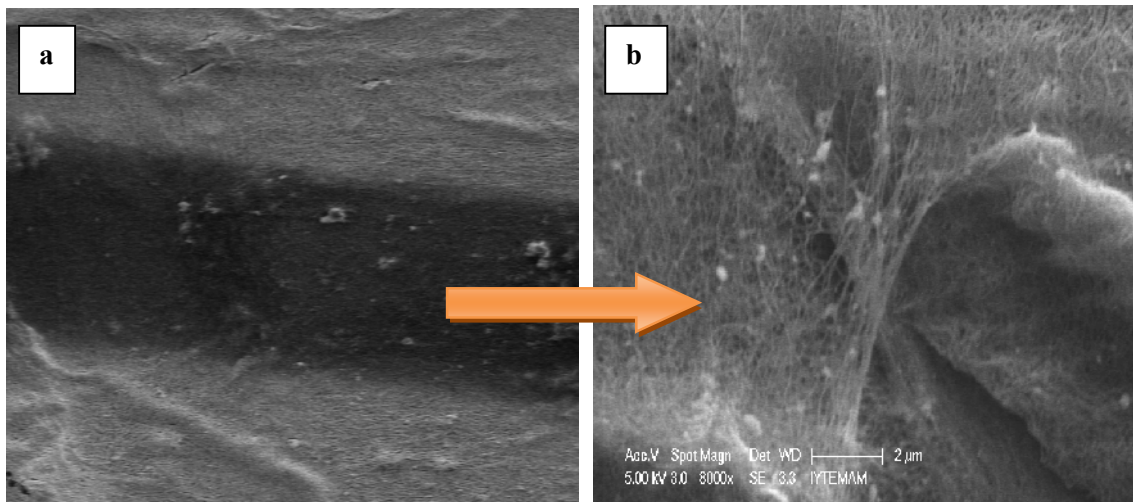


Figure 5.23. SEM images of gold electrode with CNTs with different magnifications

The first graph is belonging to the empty electrode; it shows the resistance of empty electrode with different humidity ratios.

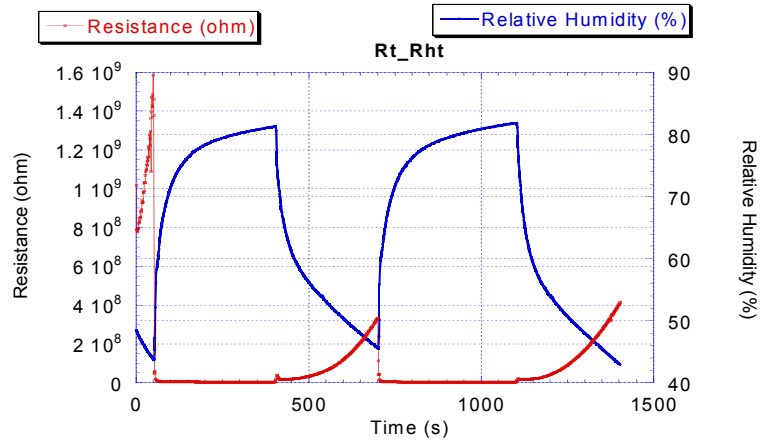


Figure 5.24. Resistance –Humidity graph of empty gold electrode

This graph shows that the resistance of empty gold electrode is nearly $3 \times 10^8 \Omega$ with roughly %55 humidity ratio and when the humidity ratio is decreased the resistance of electrode is increased.

The first CNT, analysed electrically, was FeAlO9CNT 297. Different parameters were applied for this sample such as, taking datas at the room condition and measuring resistance for long time to see if there is a changing with for a long time or not. The first graph for this sample is resistance - humidity graph.

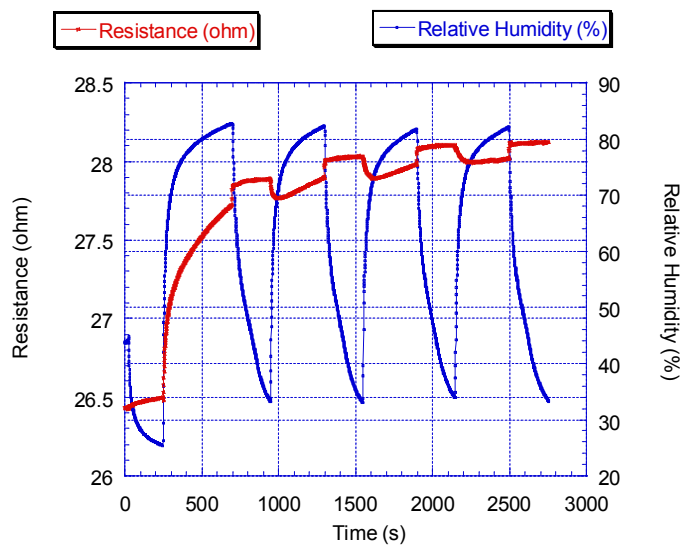


Figure 5.25. Resistance –Humidity graph of FEAlO9CNT 297

It is seen in graph that the resistance of CNTs is nearly 28 Ohm, however it is not totally true because the relation of resistance and temperature was not researched so there is no information about energy gap of CNTs. It can be said that CNTs are conductor because the resistance of electrode decreased from 3×10^8 Ohm to 28 Ohm. When humidity is roughly %80 and when the humidity is decreased the resistance is increased however, this changing is so small. It means that CNTs are not affected from humidity dramatically. The significant point is that the first coincidence of CNT and humidity shows an opposite reaction because the resistance is increased when the humidity is increased until the CNTs is filled with humidity, they shows the normal reaction. However, all the reaction and the all changing of CNTs are so small.

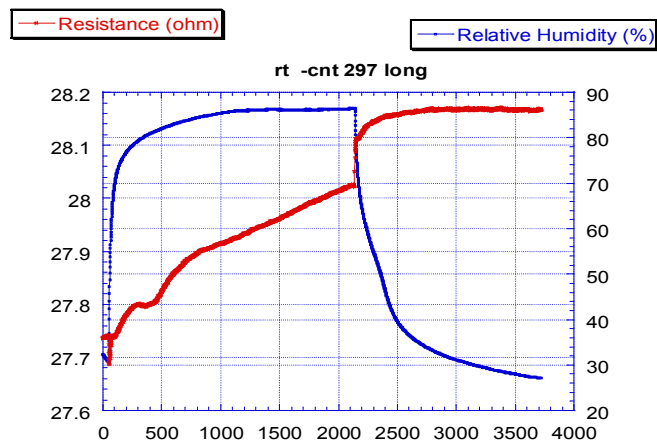


Figure 5.26. Resistance –Humidity graph of FEAlO9CNT297 for along time

The above graph shows that the applied time does not affect the resistance of CNTs because the resistance of CNT is still nearly 28 Ohm.

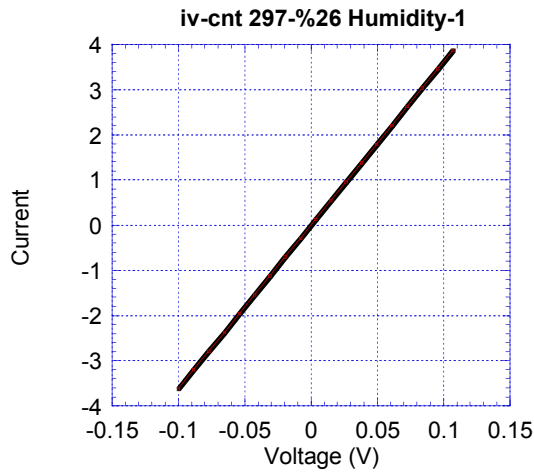


Figure 5.27. Current-Voltage (I-V) graph of FEAlO9CNT 297

The above graph is current –voltage graph and it is linear tendency. During measurement, 10 mV was applied .

Second sample is FEAlOCNT 273, the same procedure was done for this sample and the resistance humidity relation was observed and for this sample different range of humidity was applied to see the dramatical changing. The first figure, the following one, for this sample is resistance humidity graph.

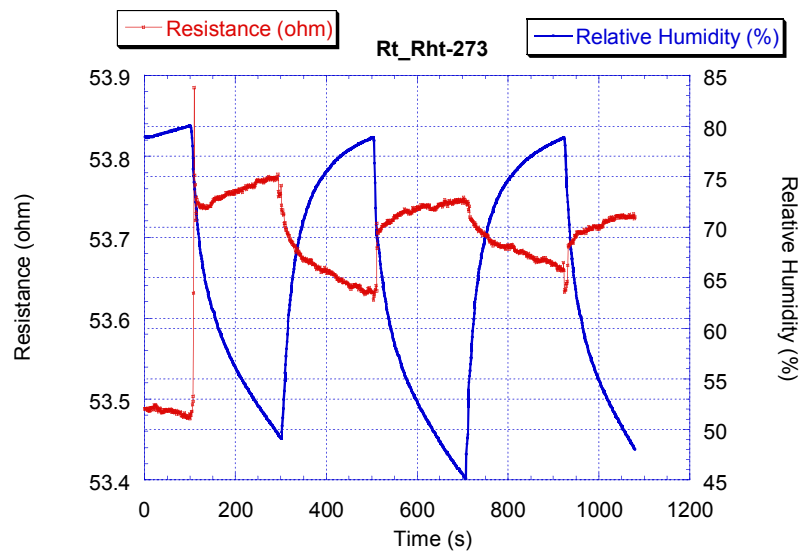


Figure 5.28 Resistance –Humidity graph of FEAlO9CNT273

The humidity is changed between %80 and %45 and the total changing for resistance is only 0.4 Ohm and the resistance of CNTs for this sample is roughly 53 Ohm. The following figure gives more information about the relation between the resistance of CNTs and the humidity.

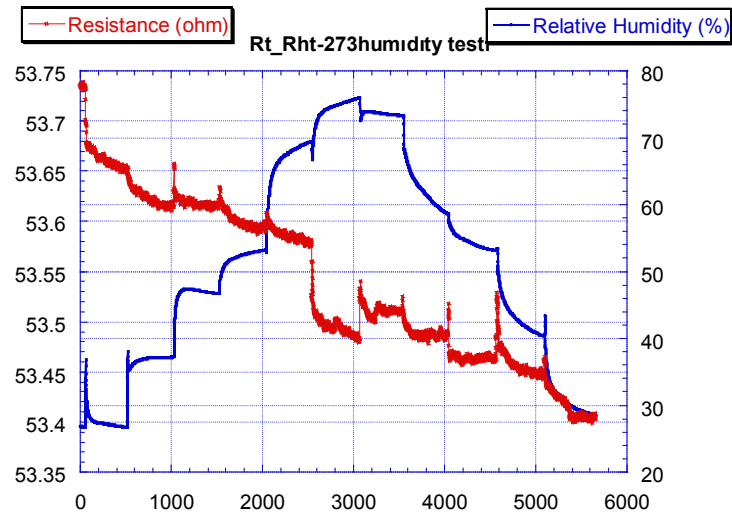


Figure 5.29. Resistance –Humidity graph of FEAlO9CNT297 with different humidity ratio

For taking this data, six different solutions were used as a humidity source and each of them has a different humidity ratio between %30 and %85. In spite of dramatical changing of humidity ratio is seen in graph, the total changing of resistance 0.35 Ohm. It shows again that humidity does not change the resistance of CNTs.

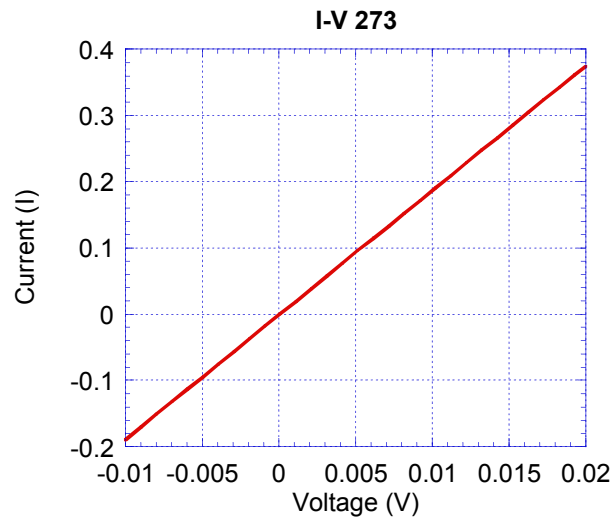


Figure 5.30. Current-Voltage (I-V) graph of FEAlO9CNT 273

The above graph is current – voltage graph of FeAlO9CNT 273, again the line is perfect. 20 mV voltage was applied to take I-V graph. The third sample is FeAlO8CNT 276 and the normal procedure was applied also for this sample and the relation between the humidity and the resistance was observed and the resistance of CNTs was measured.

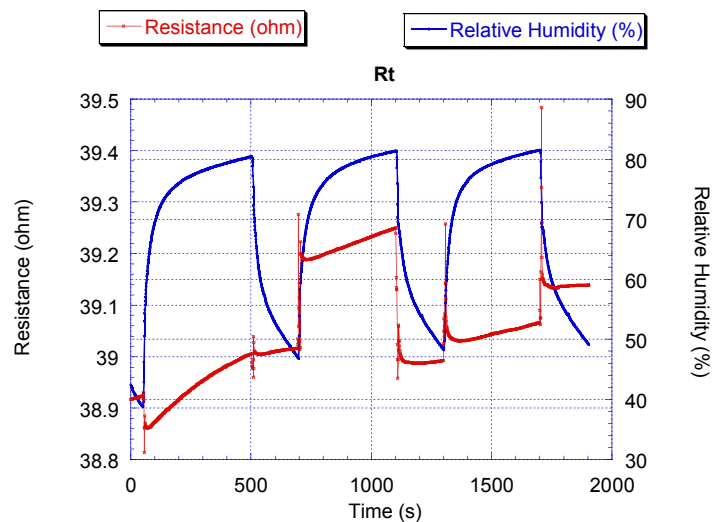


Figure 5.31. Resistance –Humidity graph of FEAlO8CNT 276

According to the graph, the resistance decreased to roughly 39 Ohm and this sample also gives the same results like the previous samples, the resistance is decreased so small with increasing humidity ratio.

The last sample is FeAlO₈CNT 283, there is no TEM image for this sample so it is not known that how many walls this CNTs have.

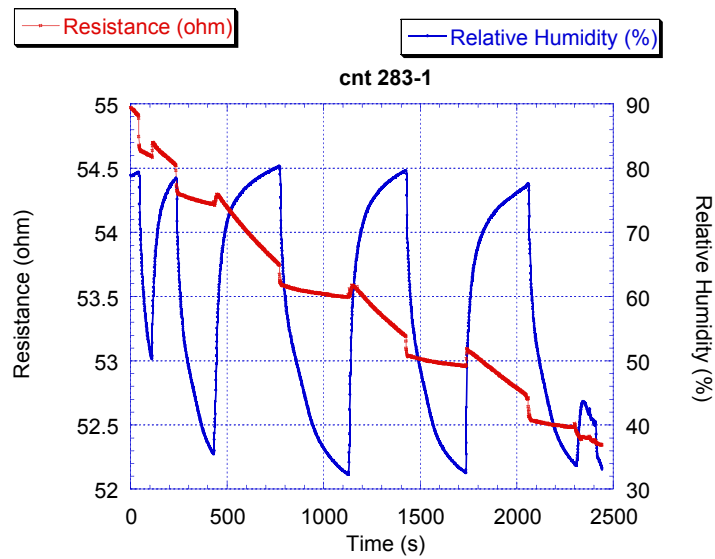


Figure 5.32. Resistance –Humidity graph of FEAlO₈CNT 283

It is realized that the resistance of the CNTs is seen nearly 52 Ohm and it means that the CNTs are metal, however it is not absolutely true because the resistivity of CNTs could not be calculated. Also, the changing ratio of humidity does not affect the resistance from this changing ratio.

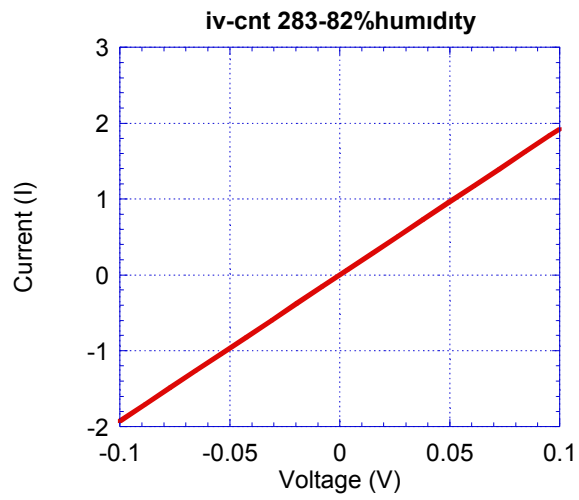


Figure 5.33. Current-Voltage (I-V) graph of FEAlO8CNT 283

This current- voltage graph was taken by applying 20 mV voltage and the line is perfect. It is not absolutely true however it can be seen that CNTs are conductor.

CHAPTER 6

CONCLUSION

In this thesis work, firstly parameters were optimized and the ideal conditions were investigated to grow vertically aligned carbon nanotubes. To optimize parameters, some significant parameters were examined and CNTs were characterized for their structural and electrical properties.

In the first part, the supporting layer effect was examined for three different hydrocarbon gas / hydrogen gas ratio. SiO_2 and Al_2O_3 were used as buffer layers to prevent the interaction between Si and metal catalyst film. One kind of sample had only one oxide layer which was Al_2O_3 the other kind of sample had both oxide layers. These samples were compared and according to results, the density of CNTs was denser on the surface of the sample which had two oxide layers. Only Al_2O_3 buffer layer was not enough to prevent the occurring metal silicide.

Moreover, the catalyst effect was performed for three different temperature value such as $650\text{ }^\circ\text{C}$, $700\text{ }^\circ\text{C}$, $750\text{ }^\circ\text{C}$. For this part, Iron and Cobalt catalyst thin film were compared at these temperatures. The results showed that Fe nanoparticles were more reactive with ethylene gas according to Cobalt particles. The density of CNTs was increased by using Fe and also increasing temperature. The diameters of CNTs were smaller when Fe catalyst nanoparticles were used.

Furthermore, the other significant parameter was Hydrogen pretreatment time effect on growth of CNTs. At high temperature and after Hydrogen pretreatment process, catalyst thin films reformed to catalyst nanoparticles. The diameters and the density of nanoparticles directly affected the diameters and density of CNTs. Seven different time parameters were examined for this part. After performing 0, 5, 10, 15, 20, 25, 30 minutes Hydrogen treatment, the diameters and density of CNTs were compared. According to results, the diameters of nanoparticles decreased until the treatment time was 20 minutes. After 20 minutes, the catalyst particles started to agglomerate.

Finally, two point contact mode was used to measure the resistance of CNTs. The resistance of CNTs was not measured absolutely because there was no opportunity

to research the relation between resistance and temperature. Hence, there is no information about the energy gap of CNTs. Only, it can be said that, CNTs conduct electricity because they reduce the resistance of empty gold electrode from 3×10^8 Ohm to nearly 28-53 Ohm. The resistance of carbon nanotubes increased with decreasing humidity except for the first coincidence of CNTs and humidity. The significant point is that the first coincidence of CNT and humidity shows an opposite reaction because the resistance is increased when the humidity is increased until the CNTs are filled with humidity. However, humidity did not change the resistance of CNTs dramatically.

REFERENCES

- Ago, H., K. Murata, M. Yumura, J. Yotani, and S. Uemura. 2003. Ink-jet printing of nanoparticle catalyst for site-selective carbon nanotube growth. *Applied Physics Letters* 82:811-819.
- Ago, H., T. Komatsu, S. Ohshima, Y. Kuriki, and M. Yumura. 2000. Dispersion of metal nanoparticles for aligned carbon nanotube arrays. *Applied Physics Letters* 77:79-82.
- Aksak, M. 2008. *Growth and Characterization of Carbon Nanotubes by Termal Vapor Deposition Method*. Izmir Institue of Technology.
- Alexandrou, I., H. Wang, N. Sano, and G. A. J. Amaratunga. 2004. Structure of carbon onions and nanotubes formed by arc in liquids. *Journal of Chemical Physics* 120:1055-1058.
- Ando, Y., X. Zhao, T. Sugai, and M. Kumar. 2004. Growing carbon nanotubes. *Materials Today* 1369(7):22-29.
- Arthur, J. and A. Cho. 1973. Adsorption and desorption kinetics of Cu and Au on (0001) graphite. *Surface Science* 36:64-660.
- Avouris, P. 2002. Carbon nanotube electronics. *Chemical Physics* 28:429-445.
- Baddour, C. and C. Briens. 2005. Carbon Nanotube Synthesis : a review R3. *Internation Journal of Chemical Reactor Engineering* 3 :20-22
- Baker, R.T.K. and P.S. Harris. 1978. *Formation of filamentous carbon in chemistry and physics of carbon 14*. New York: Marcel Dekker.
- Baker, R.T.K., M.A. Barber, P.S. Harris, F.S. Feates, and R.J. Waite. 1972. Nucleation and growth of carbon deposits from the nickel catalyzed decomposition of acetylene. *Journal of Catalysis* 26:51-62.
- Bernstein, E. 1990. Atomic and molecular clusters. *Elsevier Science B.V*, Newyork
- Bethune, D.S., C.H. Kiang, M.S. Vries, G. Gorman, R. Savoy, J. Vazquez, and R.Beyers. 1993. Cobalt-catalyzed growth of CNTs with single atomic layer walls. *Nature* 363:605-607.

- Bhuyan, H., M. Favre, E. Valderrama, G. Avaria, H. Chuaqui, I. Mitchell, E. Wyndham, R. Saavedra, and M. Paulraj. 2007. Formation of hexagonal silicon carbide by high energy ion beam irradiation on Si(100) substrate. *Journal of Physics D: Applied Physics* 40:127-131.
- Bonard, J.M. 2006. Carbon nanostructures by hot filament chemical vapor deposition : growth, properties, applications. *Thin Solid Films* 501 :8-14.
- Cheng, H.M., S.F. Li, G. Pan, H.Y. Pan, L.L. He, and X. Sun. 1998. Large-scale and low-cost synthesis of single-walled carbon nanotubes by the catalytic pyrolysis of hydrocarbons. *Applied Physics Letters* 72:3282-3284.
- Cheung, C.L., A. Kurtz, H. Park, and C.M. Lieber. 2002. Diameter-controlled synthesis of carbon nanotubes. *Journal of Physical Chemistry B* 106:2429-2433.
- Cho, Y.S., G.S. Choi, S.Y. Hong, and D. Kim. 2002. Carbon nanotube synthesis using a magnetic fluid via thermal chemical vapor deposition. *Journal of Crystal Growth* 243:224-229.
- Choi, Y.C., Y.M. Shin, Y.H. Lee, B.S. Lee, G.S. Park, and W.B. Choi. 2000. Controlling the diameter, growth rate, and density of vertically aligned carbon nanotubes synthesized by microwave plasma-enhanced chemical vapor deposition. *Applied Physics Letters* 76:2367-2372.
- Colbert D.T., M. Zhang, S.M. McClure, P. Nikolaev, Z. Chen, J.H. Hafner, D.W. Owens, P.G. Kotula, C.B. Carter, J.H. Weaver, A.G. Rinzler, and R. E. Smalley. 1994. Growth and sintering of fullerene nanotubes. *Science* 266:1218-1222.
- Colomer, J.F., J.F. Bister, I. Willems, Z. Konya, A. Fonseca, and G. V. Tendeloo. 1999. Synthesis of single-wall carbon nanotubes by catalytic decomposition of hydrocarbons. *Chemical Communications* 14:1343-1344.
- Colomer, C., S. Stephan, G. Lefrant, V. Tendeloo, I. Willems, and Z. Kónya. 2000. Large-scale synthesis of single-wall carbon nanotubes by catalytic chemical vapor deposition (CCVD) method. *Chemical Physics Letters* 317:83-89.
- Cui, H., O. Zhou, and B.R. Stoner. 2000. Deposition of aligned bamboo-like carbon nanotubes via microwave plasma enhanced chemical vapor deposition. *Journal of Applied Physics* 88(10):6072-6077.
- Cui, H., G. Eres, J.Y. Hawe. 2003. Growth behavior of carbon nanotubes on multilayered metal catalyst film in CVD. *Chemical Physics Letters* 374 : 222-228.

- Dai H. 2002. Carbon nanotubes: opportunities and challenges. *Surface Science* 500:218-241.
- Deck, C.P. and K. Vecchio. 2006. Prediction of Carbon nanotube growth success by the analysis of carbon-catalyst binary phase diagrams. *Carbon* 44:267-275.
- Dresselhaus, Mildred S., Gene Dresselhaus, and Phaedon Avouris, eds. 2001. *Carbon nanotubes: synthesis, structure, properties, and applications*. Berlin: Springer Publishers.
- Dresselhaus, M.S., G. Dresselhaus, A. Jorio, A.G.S. Filho, and R. Saito. 2002. Raman Spectroscopy on isolated single wall carbon nanotubes. *Carbon* 40:2043-2061.
- Dresselhaus, M.S., Y. M. Lin, O. Rabin, A. Jorio, A.G. Souza, M.A. Pimenta, R. Saito, G.G.Samsonidze, and G. Dresselhaus. 2003. Nanowires and nanotubes. *Materials Science and Engineering C* 23(1-2):129-140.
- Duesberg, G.S., A.P. Graham, M. Liebau, R. Seidel, E. Unger, F. Kreupl, and W.Hoenlein. 2003. Growth of isolated carbon nanotubes with lithographically defined diameter and location. *Nano Letters* 3(2):257-259.
- Dupuis, A.C. 2005. The catalyst in the CCVD of carbon nanotubes: a review. *Progress in Materials Science* 50(8):929-961.
- Ebbesen, T.W. 1994. Carbon nanotube. *Annual Review Materials* 24:235-264.
- Feldman, Leonard C. and James W. Mayer. 1986. *Fundamentals of surface and thin film analysis*. New Jersey: PTR Prentice-Hall, Inc.
- Gaskell, M. 1999. Large Scale CVD Synthesis of Single Walled Carbon Nanotubes. *Journal Physics Chemistry* 103: 6484-6492
- Guo, T., P. Nikolaev, A. Thess, D.T. Colbert, and R.E. Smalley. 1995. Catalytic growth of single-walled nanotubes by laser vaporization. *Chemical Physics Letters* 243:49-54.
- Guo, T, P. Nikolaev, A.G. Rinzler, D. Tomanek, D. T. Colbert, and R.E, Smalley. 1995. Self-assembly of tubular fullerenes. *Journal of Physical Chemistry* 99(27): 10694-10697.
- Guan, L., K. Suenaga, and S. Iijima. 2008. Smallest carbon nanotube assigned with atomic resolution accuracy. *Nano Letters* 8(2):459-462.

- Hamada, N., S. Sawada, A. Oshiyama. 1992. New one – dimensional conductors: graphitic microtubules. *Physics Review Letters* 68 : 1579 -1581.
- Hansen, Max and Kurt Anderko.1958.*Constitution of binary alloys* .NewYork: McGraw-Hill.
- Harris, P. J. F. 2007.Solid state growth mechanisms for carbon nanotubes.*Carbon* 45:229-239.
- Hart, J. 2006. *Chemical, mechanical, and thermal control of substrate-bound carbon nanotube growth*. Extended of abstract of doctoral thesis.
- Hernadi, K., A. Fonseca, J.B. Nagy, D. Bernaerts, A. Fudala, and A.A. Lucas. 1996. Catalytic synthesis of carbon nanotubes using zeolite support. *Zeolites* 17:416-423.
- Heer, W.A. and D. Ugrate. 1993. Carbon onions produced by heat treatment of carbon soot and their relation to the 217.5 nm interstellar absorption feature. *Chemical Physics Letters* 207:480-486.
- Hone, J., W. Whitney, C. Piskoti, and A. Zettle. 1999. Thermal conductivity of single walled carbon nanotubes. *Physical Review B* 59(4):2514-2516.
- Hongo, H., M. Yudasaka, T. Ichihashi, F. Nihey, and S. Iijima. 2002. Chemical vapor deposition of single-wall carbon nanotubes on iron-fill-coated sapphiresubstrates. *Chemical Physics Letters* 361:349-354.
- Hongo, H., F. Nihey, T. Ichihoshi. 2003. Support materials based on converted aluminum films for chemical vapor deposition growth of single- wall carbon nanotubes. *Chemical Physics Letters* 380: 15164.
- Huang, Z.P., J.W. Xu, Z.F. Ren, J.H. Wang, M.P. Siegal, and P.N. Provencio.1998. Growth of highly oriented carbon nanotubes by plasma-enhanced hot filament chemical vapor deposition. *Applied Physics Letters* 73:3845-3846.
- Huczko, A. 2002. Synthesis of aligned carbon nanotubes. *Applied Physics Letters A* 74: 617-638.
- Iijima, S. 1991. Helical microtubules of graphitic carbon. *Nature* 354:56-58.
- Iijima, S. and T. Ichihashi. 1993. Single-shell carbon nanotubes of 1 nm diameter. *Nature* 363:603-605.

- Ivanov, V., J. B. Nagy, P. Lambin, A. Lucas, X.F. Zhang, and D. Bernaerts. 1994. The study of carbon nanotubules produced by catalytic method. *Chemical Physics Letters* 223:329-335.
- Ivchenko, E.L. and B. Spivak. 2002. Chirality effects in carbon nanotubes. *Physical Review B* 66(15):155404-155413.
- Jiao, J. and S. Seraphin. 2000. Single-walled tubes and encapsulated nanoparticles comparison of structural properties of carbon nanoclusters prepared by three different methods. *Journal of Physics and Chemistry of Solids* 61:1055-1067.
- Jodin, L., A.C. Dupuis, E. Rouviere, P. Reiss. 2006. Influence of the Catalyst Type on the Growth of Carbon Nanotubes via Methane Chemical Vapor Deposition. *Journal Physics Chemistry B* 110: 7328-7333.
- Journet, C. and P. Bernier. 1998. Production of carbon nanotubes. *Applied Physics A* 67:1-9.
- Jung, M. and K. Young. 2001. Growth of carbon nanotubes by chemical vapor deposition. *Diamond and Related Materials* 10: 1235-1240.
- Jung, Y. 2003. Mechanism of selective growth of carbon nanotubes on SiO₂/Si patterns. *Nano Letters* 3(4): 561- 564.
- Kajiura, H., S. Tsutsui, K. Kadono, M. Kakuta, M. Ata, and Y. Murakami. 2003. Hydrogen storage capacity of commercially available carbon materials at room temperature. *Applied Physics Letters* 82(7):1105-1110.
- Kataura, H., Y. Kumazawa, Y. Moniwa, Y. Ohtsuka. 2000. Diameter control of single walled carbon nanotubes. *Carbon* 38 (11-12): 1691- 1697.2000.
- Kelly, P.J., R.D. Arnell. Magnetron sputtering : a review of recent developments and applications. *Vacuum* 56 : 159-172.
- Kiang, C. H. 2000. Carbon rings and cages in the growth of single-walled carbon nanotubes. *Journal of Chemical Physics* 113(11):4763-4767.
- Klinke, C., J.-M. Bonard, and K. Kern. 2001. Comparative study of the catalytic growth of patterned carbon nanotube films. *Surface Science* 492:195-201.
- Kong, J., A.M. Cassell, and H. Dai. 1998. Chemical vapor deposition of methane for single-walled carbon nanotubes. *Chemical Physics Letters* 292(4):567-574.

- Kroto, H.W., J.R. Heath, S.C. O'Brien, R.F. Curl, R.E. Smalley. 1985. C₆₀: buckminsterfullerene. *Nature* 318:162-163.
- Kukovecz, A., Z. Kónya, N. Nagaraju, I. Willems, A. Tamási, A. Fonseca, J.B. Nagy, I. Kiricsi. 2000. Catalytic synthesis of carbon nanotubes over Co, Fe and Ni containing conventional and sol-gel silica-aluminas. *Physical Chemistry Chemical Physics* 2:3071-3076.
- Kukovitsky, E.F., S.G. L'vov, N.A. Sainov, V.A. Shustov, and L.A. Chernozatonskii. 2002. Correlation between metal catalyst particle size and carbon nanotube growth. *Chemical Physics Letters* 355:497-503.
- Laurent, C., E. Flahaut, A. Peigney, and A. Rousset. 1998. Metal nanoparticles for the catalytic synthesis of carbon nanotubes. *New Journal of Chemistry* 1229-1237.
- Lee, C. J., J. Park, and J.A. Yu. 2002. Catalyst effect on carbon nanotubes synthesized by thermal chemical vapor deposition. *Chemical Physics Letters* 360:250-255.
- Lee C.J., J. Park, Y. Huh, and J.Y. Lee. 2001. Temperature effect on the growth of CNTs using thermal chemical vapor deposition. *Chemical Physics Letters* 343: 33-38.
- Li, Y., W. Kim, Y. Zhang, M. Rolandi, D. Wang, and H. Dai. 2001. Growth of single walled carbon nanotubes from discrete catalytic nanoparticles of various sizes. *Journal of Physical Chemistry B* 105:11424-11431.
- Li, W.Z., D.Z. Wang, S.X. Yang, J.G. Wen. 2001. *Chemical Physics Letters* 335:141-149.
- Makris, D., L. Giorgi, R. Giorgi. 2005. CNT growth on alumina supported nickel catalyst by CVD. *Diamond and Related Material* 14:815-819.
- Marty, L., V. Bouchiat, A.-M. Bonnot, M. Chaumont, T. Fournier, S. Decossass, and S. Rocha. 2002. Batch processing of nanometer-scale electrical circuitry based on in-situ grown single-walled carbon nanotubes. *Microelectronic Engineering* 61:485-489.
- Mattavi, C. 2008. *Journal Physics Chemistry. C*, 112, 12207-12213.
- Matthews, K. and M. Lemoitre. 2006. Growth modes of carbon nanotubes on metal substrate. *Journal of Applied Physics* 100: 044309.
- Merkoci, A. 2006. Carbon nanotubes in analytical sciences. *Microchimica Acta* 152:157-174.

- Moisala, A., A.G. Nasibulin, and E.I. Kapauppinen. 2003. The role of metal nanoparticles in the catalytic production of single-walled carbon nanotubes. *Journal of Physics: condensed matter* 15:3011-3035.
- Monthieux, M. and V. L. Kuznetsov. 2006. Who should be given the credit for the discovery of carbon nanotubes. *Carbon* 44(9):1621-1623.
- Moshkalyov, S. and C. Betonzo. 2004. Growth of multi walled carbon nanotubes by chemical vapor deposition. *Revista Brasileira de Aplicações de Vacuo* 23(2): 47-48.
- Murokami, Y., S. Chiashi, Y. Miyauchi, M. Hu, M. Ogura, T. Okubo, S. Moruyama. 2004. *Chemical Physics Letters* 385: 298.
- Nikolaev, P., M. Bronikowski, R. Bradley, F. Rohmund, D. Colbert, K. Smith, and R.E. Smalley. 1999. Gas-phase catalytic growth of single-walled carbon nanotubes from carbon monoxide. *Chemical Physics Letters* 313(1):91-97.
- Noda, S., H. Sugime, T. Osawa, Y. Tsuji, S. Chiashi, Y. Murokami, S. Maruyama. 2006. *Carbon* 44: 1414.
- Oberlin A, M. Endo, T. Koyama. 1976. Filamentous growth of carbon through benzene decomposition. *Journal of Crystal Growth* 32:335-349.
- O'Connor Daniel. J., Brett A. Sexton, Roger St. C. Smart. 2003. *Surface analysis methods in materials science*. New York: Springer Publishers.
- Odom, T., J. Huang, P. Kim, M. Lieber. 1998. Atomic structure and electronic properties of single-walled carbon nanotubes. *Nature* 391 : 62-64.
- Pan, S.S., Z.W. Xie, B.H. Chang, L.F. Sun, W.Y. Zhou, and G. Wang. 1999. Direct growth of aligned open carbon nanotubes by chemical vapor deposition. *Chemical Physics Letters* 299:97-102.
- Park J.B, G.S. Choi, Y.S. Cho, S.Y. Hong, D. Kim, S.Y. Choi, J.H. Lee, K. Cho. 2002. Characterization of Fe-catalyzed carbon nanotubes grown by thermal chemical vapor deposition. *Journal of Crystal Growth* 244:211-217.
- Popov, V.N. 2004. Carbon nanotubes: properties and applications. *Materials Science and Engineering Reports* 43:61-102.
- Qingwen, L., Y. Hao, C. Yan, Z. Jin, L. Zhongfan. 2002. A scalable CVD synthesis of high purity single walled carbon nanotubes with porous MgO as support material. *Journal of Materials Chemistry* 12:1179-1183.

- Radushkevich LV, V.M. Lukyanovich. 1952. O strukture ugleroda, obrazujucegosja priTermiceskom razlozenii okisi ugleroda na zeleznom kontakte. *Zurn Fisic Chim*26: 88-95.
- Reich, S., C. Thomsen, and J. Maultzsch. 2004. *Carbon nanotubes: basic concepts and physical properties*. Berlin: Wiley-VCH.
- Ren, Z.F., Z.P. Huang, J.W. Xu, J.H. Wang, P. Bush, and M.P. Siegal.1998. Synthesis of large arrays of well-aligned carbon nanotubes on glass. *Science* 282:1105-1107.
- Richardson, J. T. 1989. *Principles and catalyst development*. New York: Plenum Press.
- Roth, Siegmur and David Carroll. 2004. *One dimensional Metals*. Berlin: Wiley-VCH.
- Rotkin, Slava V. and Shekhar Subramoney, eds. 2005. *Applied physics of carbon nanotubes: fundamentals of theory, optics, and transport devices*. New York: Springer Publishers.
- Rummeli M.H., E. Borowiak-Palen, T. Gemming, T. Pichler, M. Knupfer, and M.Kalbac. 2005. Novel catalysts, room temperature and the importance of oxygen for the synthesis of single-walled carbon nanotubes. *Nano Letters* 5(7):1209-1215.
- Saito, R., M. Fujita, G. Dresselhaus, M.S. Dresselhaus. 1992. Electronic structure of chiral graphene tubules. *Applied Physics Letters* 60(18):2204-2207.
- Saito Y, M. Okuda, N. Fujimoto, T. Yoshikawa, M. Tomita, T. Hyashi. 1994. Single wall carbon nanotubes growing rapidly from Ni fine particles formed by arc evaporation. *Japan Journal of Applied Physics Part 2- Letters* 33:526-529.
- Saito, Riichiro, Gene Dresselhaus, and Mildred S. Dresselhaus. 1998. *Physical properties of carbon nanotubes*. London: Imperial College Press.
- Satishkumar, B.C., A. Govindaraj, R. Sen, and C.N.R. Rao. 1998. Single-walled nanotubes by the pyrolysis of acetylene-organometallic mixtures. *Chemical Physics Letters* 293:47-52.
- Sen, R., A. Govindaraj, and C.N.R. Rao. 1997. Carbon nanotubes by the metallocene route. *Chemical Physics Letters* 267:276–280.

- Seshan, Krishna. 2002. *Handbook of thin film deposition processes and techniques, principles, methods, equipments, and applications*. New York: William Andrew Publishing.
- Shanov V., Y.H. Yun, M.J. Schulz. 2006. Synthesis and characterization of carbon nanotube materials. *Journal of the University of Chemical Technology and Metallurgy* 41(4):377-390.
- Siegal, M.P., D.L. Overmyer, and P.P. Provencio. 2002. Precise control of multiwall carbon nanotube diameters using thermal chemical vapor deposition. *Applied Physics Letters* 80:2171-2176.
- Seidel, R., G.S. Duesberg, E. Unger, A.P. Graham, M. Liebau, and F. Kreupl. 2004. Chemical vapor deposition growth of single-walled carbon nanotubes at 600 °C and a simple growth model. *Journal of Physical Chemistry B* 108:1888-1893.
- Stahl, H. 2000. *Electronic Transport in Ropes of Single Wall Carbon Nanotubes*. Aachen University of Technology
- Tans, S. J., M.H. Devoret, H. Dai, A. Thess, R.E. Smalley, L.J. Geerligs, and C. Dekker. 1997. Individual single-wall carbon nanotubes as quantum wires. *Nature* 386:474-477.
- Taylor, W.J., T.Y. Tan, U. Gosele. 1993. Carbon precipitation in silicon: why is it so difficult. *Applied Physics Letters* 62(25):3336-3338.
- Teo, K.B.K., M. Chhowalla, G.A.J. Amaratunga, W.I. Milne, D.G. Hasko, G. Pirio. 2001. Uniform patterned growth of carbon nanotubes without surface carbon. *Applied Physics Letters* 79:1534-1540.
- Thostenson, E.T., Z. Ren, and T.W. Chou. 2001. Advances in the science and technology of carbon nanotubes and their composites: a review. *Composites science and Technology* 61:1899-1912.
- Tibbetts, G. 1984. Why are carbon filaments tubular. *Journal Crystal Growth* 66 : 632-638.
- Treffer G., J. Neuhiuser, G. Marx. 1997. XRD studies of SiC/Si layers on carbon substrates. *Mikrochimica Acta* 125:325-330.
- Venegoni, D., P. Serp, R. Feurer, Y. Kihn, C. Vahlas, and P. Kalck. 2002. Parametric study for the growth of carbon nanotubes by catalytic chemical vapor deposition on a fluidized bed reactor *Carbon* 40:1799-1807.

- Walker, P.L., F. Rusinko, L.G. Austin. 1959. Gas reactions of carbon. *Advances in Catalysis* 11:133-221.
- Wei, B.Q., R. Jung, Y. Ward, J. Zhang, R.Ramanath,G.and Ajayan.P.M. 2002. *Nature* 416 : 495-496.
- Weifeng, L., W. Cai, L.Yao, X. Li, Z. Yao. 2003. Effects of methane partial pressure on synthesis of single walled carbon nanotubes by chemical vapor deposition. *Journal of Materials Science* 38: 3051- 3054.
- Wright, A.C., Y. Xiong, N. Maung, S.J. Eichhorn, and R.J. Young. 2003. The influence of the substrate on the growth of carbon nanotubes from nickel clusters: an investigation using STM, FE-SEM, TEM, and Raman spectroscopy. *Material Science and Engineering C* 23:279-283.
- Xie, J. and K. Mukhopadyay. 2003. Catalytic chemical vapor deposition synthesis and electron microscopy observation of coiled CNT. *Smart Material Structure* 2:744-748.
- Yacaman, M.J., M.M. Yoshida, L. Rendon, and J.G. Santiesteban. 1993. Catalytic growth of carbon microtubules with fullerene structure. *Applied Physics Letters* 62:202-207.
- Yamada, T., T. Nanomi, K. Hata, D. Futuba, K. Mizuno, J. Fan, M. Yudasaka, M.Yumura, S. Iijima. 2006. *Nature Nanotechnology* 1: 131.
- Yao,Y. Synthesis of carbon nanotubes films by thermal CVD in the Presence of supported catalyst particles. 2004. *Kluwer Academic Publishers*.
- Yi, W., L. Lu, Z. Dian-lin, Z.W. Pan, S.S. Xie. 1999. Linear specific heat of carbon nanotubes. *Physical Review B* 59 (14):9015-9018.
- Yu, H. and Q. Zhang . 2006. Effect of the reaction atmosphere on the diameter of single walled nanotubes produced by CVD. *Carbon* 44 :1706- 1712.
- Yudasaka, M., R. Kikuchi, T. Matsui, O. Yoshimasa, and S. Yoshimura. 1995. Specific conditions for Ni catalyzed carbon nanotube growth by chemical vapor deposition. *Applied Physics Letters* 67:2477-2482.
- Yudasaka, M., R. Kikuchi, Y. Ohki, E. Ota, and S. Yoshimura. 1997. Behavior of Ni in carbon nanotube nucleation. *Applied Physics Letters* 70:1817-1821.

- Zhang, W., Y. Li, W. Kim, D. Wang, and H. Dai. 2002. Imaging as-grown single-walled carbon nanotubes originated from isolated catalytic nanoparticles. *Applied Physics A* 74:325-328.
- Zhang, G., D.Monn, L. Zhang. 2005.Ultra high yield growth of vertical single walled carbon nanotubes : Hidden roles of hydrogen and oxygen. *PNAS* 02:16141-16145.
- Zhu, S., C.H. Su, J.C. Cochrane, S. Lehoczky, Y. Cui, and A. Burger. 2002. Growth orientation of carbon nanotubes by thermal chemical vapor deposition. *Journal of Crystal Growth* 234:584-588.